

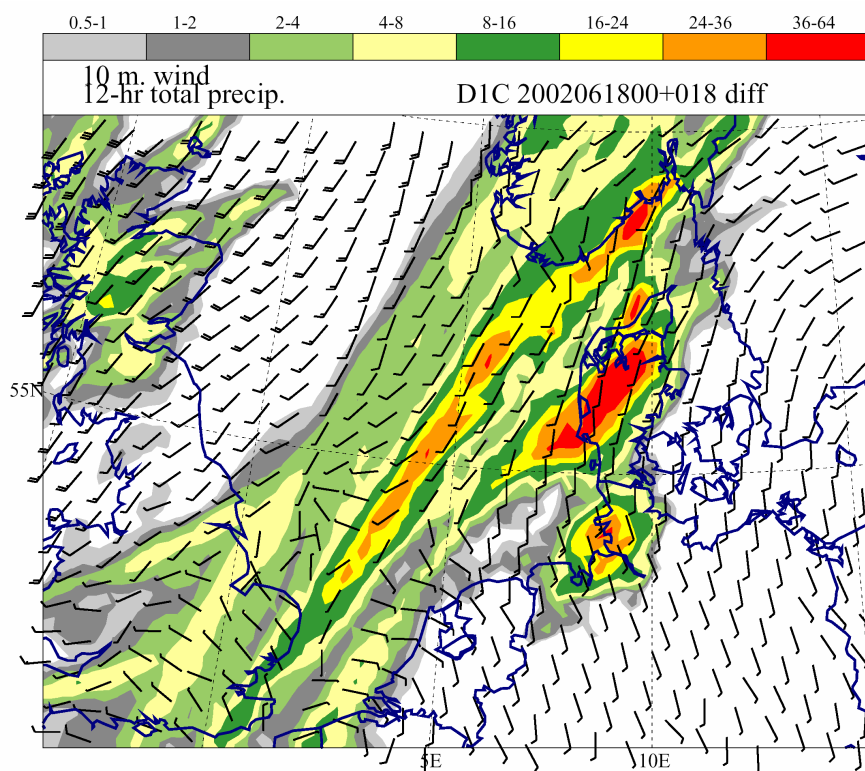
# DANISH METEOROLOGICAL INSTITUTE

## TECHNICAL REPORT

03-20

### Results from DMI-HIRLAM pre-operational tests prior to the upgrade in December 2002

Bjarne Amstrup, Kristian Sten Mogensen,  
Niels Woetmann Nielsen,  
Vibeke Huess and Jacob Woge Nielsen



COPENHAGEN 2003

**ISSN: 0906-897X (printed version)**  
**1399-1388 (online version)**

# Results from DMI-HIRLAM pre-operational tests prior to the upgrade in December 2002

Bjarne Amstrup, Kristian Sten Mogensen, Niels Woetmann Nielsen,  
Vibeke Huess and Jacob Woge Nielsen  
Danish Meteorological Institute, Copenhagen, Denmark

## Abstract

In this report we present results of the extensive testing of the pre-operational DMI-HIRLAM set-up that was operationalized on December 9th 2002. We present results both for test periods and for pre-operational runs.

The new set-up has 40 vertical levels compared to the 31 vertical levels previously used. The convection scheme (STRACO) is updated, and the upstream advection scheme previously applied to humidity and cloud water has been replaced by a centered difference scheme.

The observatorial input to the analysis system now includes NOAA16 AMSU-A data.

We test three winter periods including the December 1999 storms, and one summer period including some cases in June and July 2002 with large amounts of precipitation over Denmark.

Five cases have been checked with the storm surge model Mike21 based on forecasts from the new and old DMI-HIRLAM-E versions.

In order to maintain a very high computational stability it was found necessary to decrease the time step by about 40%.

## Introduction

A weakness of the operational DMI-HIRLAM models in the past few years has been the tendency to predict weak to moderate precipitation too frequently. This problem was somewhat reduced with the upgrade in December 2001 where, among other things, a change in the convection scheme involving an improvement in the parameterization of shallow convection was introduced (Sass, 2001). Based on parallel tests during the first quarter of 2002 (Amstrup *et al.*, 2002), a minor upgrade with a large impact on the DMI-HIRLAM operational suite took place on April 17, 2002. The upgrade concerned basically a change to using the upstream scheme for advection of humidity, cloud water (CW) and turbulent kinetic energy (TKE). This upgrade improved further on precipitation in the winter periods studied in the parallel tests as well as in the pre-operational runs made during the first quarter of 2002. However, partly due to lack of computer resources and time, no summer period was studied and subsequently it turned out that the new operational suite had difficulties with some convective situations resulting in bad forecasts of heavy precipitation. During the summer period the new NEC-SX6 was installed and many tests were made with revised STRACO schemes, and different combinations of schemes for advection of humidity, CW and TKE were studied (see Amstrup *et al.*, 2003).

Some tests were made using different sets of vertical levels leading to the conclusion that the vertical coordinate set for 40 levels proposed by Undén and Gustafsson (Undén and Gustafsson, 2001) was a good choice to replace the 31-level system previously used by DMI.

The stability in summer cases was worse with the new STRACO version with 40 vertical levels and without the upstream advection scheme on humidity and CW with the same value of the time-step. By reducing the time-step in the integration by about 40 % the new version had a stability equal to or better than the operational version. The new STRACO version is briefly described in Amstrup *et al.*, 2003.

A second step towards a better stability of the forecast model in the summer period studied was the substitution of the explicit fourth order horizontal diffusion by an implicit fourth order horizontal diffusion also used in the HIRLAM reference system Undén *et al.*, 2003. This change also reduced the noise level in the model generally measured by the domain averaged pressure tendencies ( $\text{abs}(\text{dps})/3\text{h}$ ).

Based on these investigations a new set-up was determined and put into the pre-operational suite, running in parallel with the operational suite. The test periods were run in delayed mode.

In this report the old version is named by “operational” or “old” and for the different model versions DMI-HIRLAM-G/G4A, DMI-HIRLAM-E/D1A, DMI-HIRLAM-D/D0A and DMI-HIRLAM-N/G1A. The new version is named “new” and the different model versions by DMI-HIRLAM-G-new/G4C, DMI-HIRLAM-E-new/D1C, DMI-HIRLAM-D-new/D0C and DMI-HIRLAM-N-new/G1C.

The contents of this report are: section 1 describes the differences between the old and the new version, section 2 gives an overview over the experimental set-ups including Mike21. Results are given in section 3 in terms of observation and field verification scores, Mike21 scores and case studies. Finally, main conclusions are given in section 4.

## 1. The new operational set-up

The new operational set-up differs in a number of ways from the old operational set-up. The differences are divided into 5 parts and they are briefly described in the following sections. Further details concerning the DMI-HIRLAM system can be found in Sass *et al.*, 2002.

### 1.1. Number of levels increased from 31 to 40

One of the major changes was the increase in the number of vertical levels from 31 to 40. The vertical  $\sigma$  hybrid parameters used in the 31 and 40 level set-ups (the half level parameters  $A_{k-1/2}$  and  $B_{k-1/2}$  and the full level parameters  $A_k$  and  $B_k$ ) are given in Table 1. For example the pressure at the coordinate half level surfaces is given from the following expression using  $A_{k-\frac{1}{2}}$  and  $B_{k-\frac{1}{2}}$  ( $k = 1, \dots, N + 1$ ) and the surface pressure  $p_s$ :

$$p_{k-\frac{1}{2}} = A_{k-\frac{1}{2}} + B_{k-\frac{1}{2}} p_s$$

The full levels are shown schematically in Figure 1. The lowest level is approximately the same in the two sets whereas the uppermost full level is lifted from 12.5 hPa to 10.03 hPa in the new set-up. The distribution of the levels are similar in the two set-ups, with the highest density of levels in the lower troposphere.

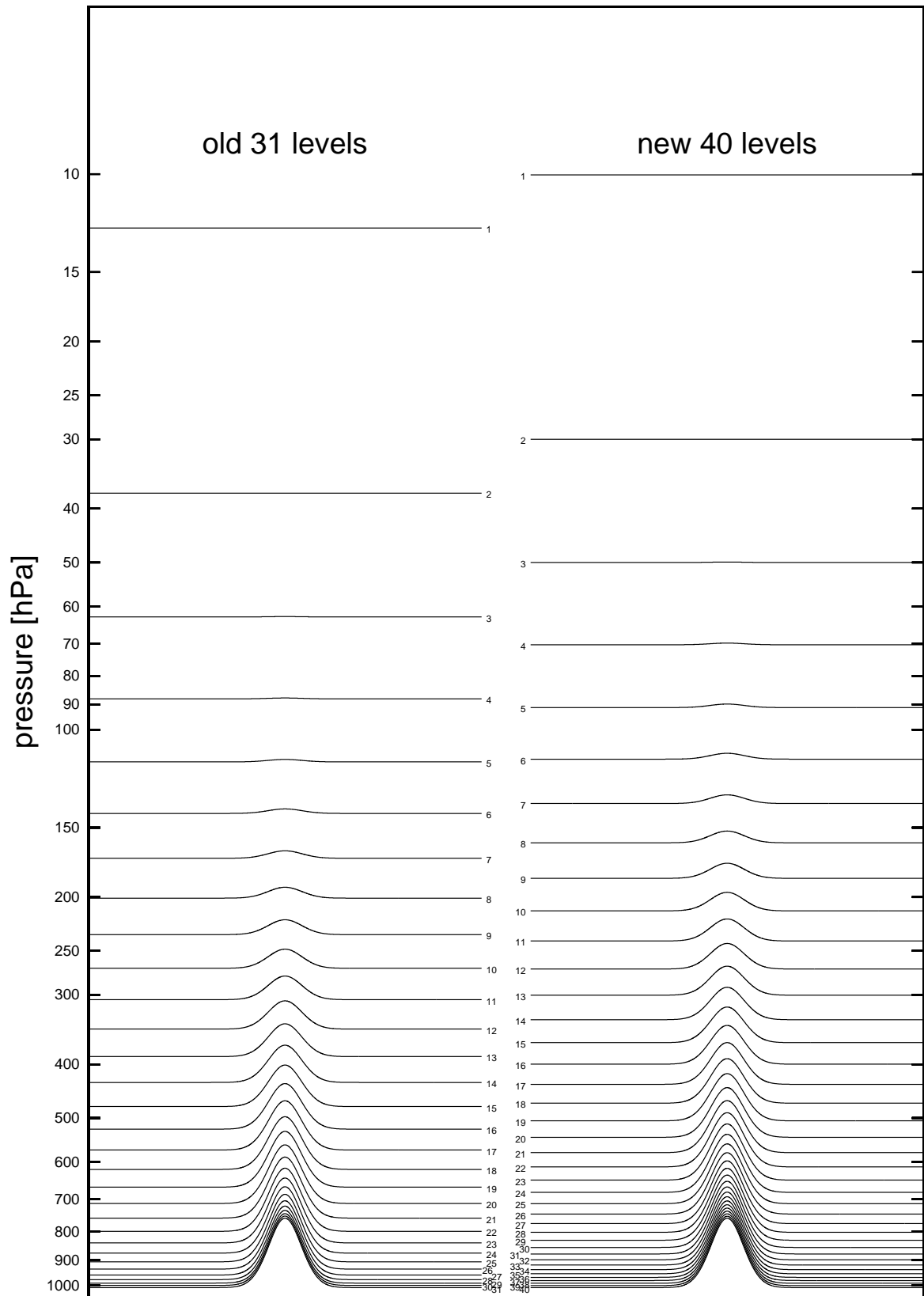


**Figure 1:** Schematical plot of vertical “distribution” of full model levels for the old 31 vertical level (left) and for the new 40 level (right).

**Table 1:** Full and half level  $\sigma$  hybrid coordinates for the new and old set-ups.

$k$	$A_k$ (old)	$B_k$ (old)	$A_{k-\frac{1}{2}}$ (old)	$B_{k-\frac{1}{2}}$ (old)	$A_k$ (new)	$B_k$ (new)	$A_{k-\frac{1}{2}}$ (new)	$B_{k-\frac{1}{2}}$ (new)
1	1250.00000	0.0000000	0.00000	0.0000000	1003.0287888	0.0000000	0.00000000	0.00000000
2	3750.00000	0.0000000	2500.00000	0.0000000	3001.4104345	0.0000000	2006.05757759	0.00000000
3	6222.63000	0.0004300	5000.00000	0.0000000	4960.2231264	0.0003962	3996.76329133	0.00000000
4	8667.89000	0.0012905	7445.26000	0.0008600	6836.0627774	0.0019211	5923.68296148	0.00079242
5	10959.46500	0.0045900	9890.52000	0.0017210	8594.7800502	0.0051903	7748.44259336	0.00304974
6	13097.36000	0.0103285	12028.41000	0.0074590	10209.9926517	0.0107089	9441.11750699	0.00733081
7	14961.25000	0.0204525	14166.31000	0.0131980	11661.8272046	0.0188780	10978.86779645	0.01408708
8	16551.12500	0.0349620	15756.19000	0.0277070	12935.8702240	0.0300004	12344.78661268	0.02366891
9	17789.83500	0.0551030	17346.06000	0.0422170	14022.3021590	0.0442874	13526.95383523	0.03633186
10	18677.38000	0.0808755	18233.61000	0.0679890	14915.1913476	0.0618649	14517.65048286	0.05224293
11	19183.67000	0.1127140	19121.15000	0.0937620	15611.9295861	0.0827797	15312.73221231	0.07148688
12	19308.71500	0.1506185	19246.19000	0.1316660	16112.7855997	0.1070057	15911.12695982	0.09407249
13	19069.54500	0.1941825	19371.24000	0.1695710	16420.5516521	0.1344501	16314.44423948	0.11993881
14	18466.16000	0.2434050	18767.85000	0.2187940	16540.2829102	0.1649602	16526.65906480	0.14896147
15	17558.90000	0.2970805	18164.47000	0.2680160	16479.0979110	0.1983290	16553.90675567	0.18095902
16	16347.75500	0.3552100	16953.33000	0.3261450	16246.0194150	0.2343019	16404.28906623	0.21569908
17	14928.65000	0.4159140	15742.18000	0.3842750	15851.8524362	0.2725826	16087.74976371	0.25290469
18	13301.58500	0.4791920	14115.12000	0.4475530	15309.0927733	0.3128400	15615.95510868	0.29226059
19	11586.49500	0.5426905	12488.05000	0.5108310	14631.8208060	0.3547139	15002.23043794	0.33341944
20	9783.38000	0.6064090	10684.94000	0.5745500	13835.6122367	0.3978215	14261.41117411	0.37600830
21	8020.75000	0.6677975	8881.82000	0.6382680	12937.4200060	0.4417636	13409.81329939	0.41963462
22	6298.61000	0.7268560	7159.68000	0.6973270	11955.4332954	0.4861312	12465.02671268	0.46389262
23	4734.72000	0.7811920	5437.54000	0.7563850	10908.9203581	0.5305114	11445.83987802	0.50836986
24	3329.08000	0.8308055	4031.90000	0.8059990	9817.9953899	0.5744935	10372.00083822	0.55265285
25	2165.52000	0.8738955	2626.26000	0.8556120	8703.3833642	0.6176761	9263.98994152	0.59633421
26	1244.04000	0.9104625	1704.78000	0.8921790	7586.1124193	0.6596725	8142.77678679	0.63901802
27	587.47500	0.9398060	783.30000	0.9287460	6487.1289209	0.7001174	7029.44805180	0.68032690
28	195.82500	0.9619255	391.65000	0.9508660	5426.9118843	0.7386733	5944.80979003	0.71990793
29	0.00000	0.9778090	0.00000	0.9729850	4424.9836261	0.7750364	4909.01397857	0.75743866
30	0.00000	0.9874570	0.00000	0.9826330	3499.3583700	0.8089431	3940.95327361	0.79263406
31	0.00000	0.9961405	0.00000	0.9922810	2665.9751351	0.6596725	3057.76346642	0.82525205
32			0.00000	1.0000000	1938.0393156	0.7001174	2274.18680381	0.85510040
33					1325.3184171	0.7386733	1601.89182737	0.88204274
34					833.3805104	0.7750364	1048.74500687	0.90600465
35					462.8203921	0.8089431	618.01601383	0.92698038
36					208.4135269	0.9526841	307.62477035	0.94503868
37					58.2347915	0.9667096	109.20228347	0.96032944
38					3.6336498	0.9783701	7.26729959	0.97308980
39					0.0000000	0.9880459	0.00000000	0.98365033
40					0.0000000	0.9962208	0.00000000	0.99244155
41							0.00000000	1.00000000

## 1.2. Implicit horizontal diffusion

The operational version uses a linear fourth order explicit horizontal diffusion scheme with the parameter AK4 set to  $1.66 \times 10^{14}$ . The new version uses a 4th order implicit horizontal diffusion scheme with the parameter CDIF set to 1.2. For DMI-HIRLAM-G these values are equivalent and for DMI-HIRLAM-E the CDIF value corresponds to a value of AK4 which is 100 times smaller than  $1.66 \times 10^{14}$  (Xiaohua Yang, private communication). For further details concerning the differences between explicit and implicit horizontal diffusion, see Undén *et al.*, 2003; Sass *et al.*, 2002.

### 1.3. Modifications to the STRACO scheme

Some modifications have also been done to the convection scheme STRACO (Sass, 2001; Sass and Yang, 2002; Amstrup *et al.*, 2003). A detailed description of the entire cloud scheme can be found in Sass, 2002.

### 1.4. Reduction of time steps

As a consequence of a) enhanced convection in the revised STRACO scheme, b) reduced stability due to increased vertical resolution, and c) reduced stability in going from upstream to centered difference advection of  $q$  and CW, the dynamics time step was reduced for all models:

	G	E	D	N
Old time step	240 s	100 s	36 s	100 s
New time step	150 s	60 s	25 s	60 s

The physics time step was reduced similarly.

### 1.5. Use of NOAA16 AMSU-A data in the 3D-VAR analysis

All the runs for the new set-up except for the December 1999+ period have used NOAA16 AMSU-A (Advanced Microwave Sounding Unit-A) radiation data in the 3D-VAR analysis system (see, e.g., Amstrup, 2003; Schyberg *et al.*, 2003 for further details) with RTTOV (Radiative Transfer model for TOVS) version 7. Version 7 of the RTTOV package is needed for use of NOAA17 AMSU-A data which is not supported by version 5 of RTTOV previously used by 3D-VAR. RTTOV is the radiative forward model used for calculating brightness temperatures from model variables corresponding to the level 1c processed observational data for the AMSU-A channels.

The HIRVDA version used in the new set-up was 5.1.2 and in the old set-up version 5.0.4 was used. The main differences between versions 5.1.2 and 5.0.4 is the use of RTTOV7 instead of RTTOV5 and some bug-fixes.

## 2. Experimental set-up

The experimental set-up is based on the operational DMI-HIRLAM set-up (Sass *et al.*, 2002). All model versions in the DMI-HIRLAM system were used for both the parallel (near) real time runs and the delayed mode runs. Up to 2001 ECMWF (European Centre for Medium-Range Weather Forecasts) provided 00 and 12 UTC forecasts on a regular grid to HIRLAM member states for lateral boundary values to the outermost of the limited area model(s) in use. From 2001 the so-called Boundary Conditions Optional Project was modified to provide boundary values in frames (FRAME boundary files) covering the boundary zones four times a day. For this purpose ECMWF produces forecasts from short cut-off 3D-VAR analyses. An example showing the surface pressure content in a FRAME boundary file is given in Figure 2. For the periods where these ECMWF FRAME boundary files were available for the delayed mode runs DMI-HIRLAM-G used those in the same way as in the operational runs (see Table 2).

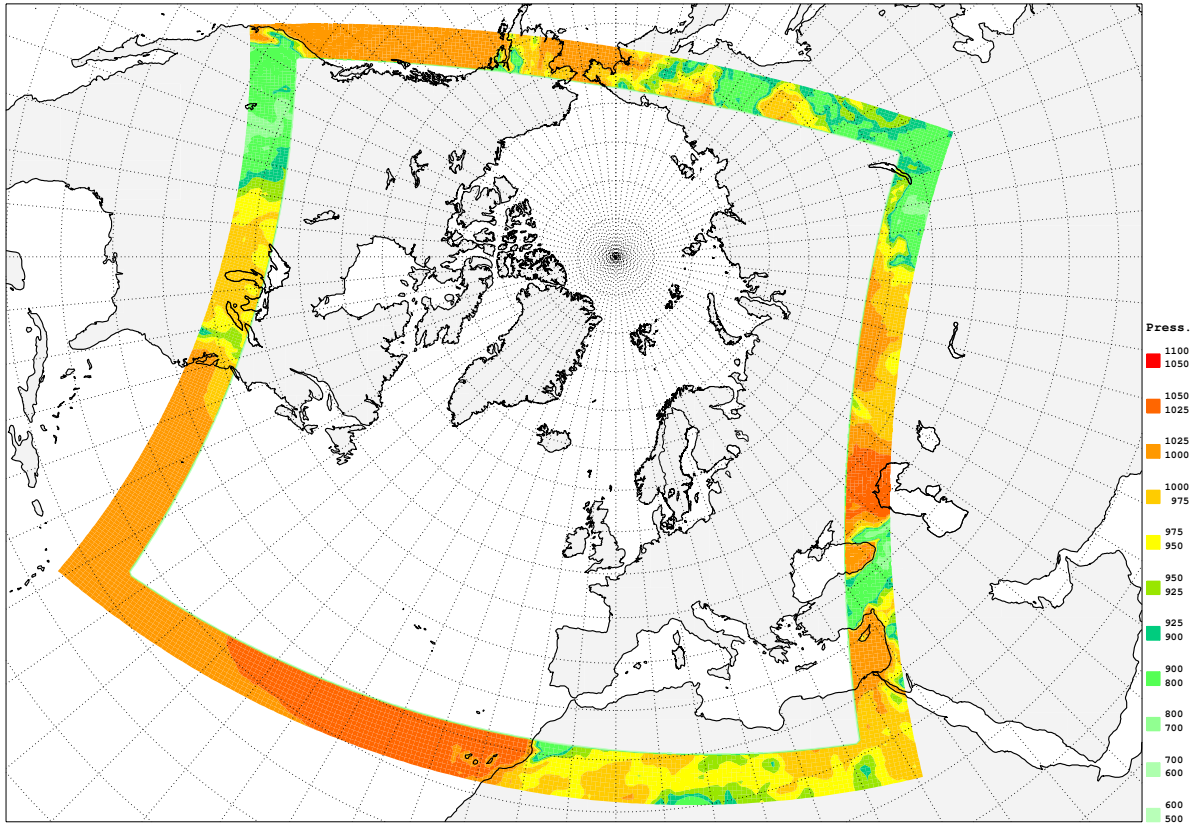


**Figure 2:** An example of the surface pressure content in an ECMWF FRAME boundary file for use with DMI-HIRLAM-G.

**Table 2:** Standard periods run for tests. Both days are included. The boundary files are for DMI-HIRLAM-G (see text) and the frequency is how often the boundary files are available.

Name of period	start day	end day	#days	Boundary files	freq.
June/July 2002	20020610	20020712	33	Rotated FRAME forecasts	3 h
January/February 2002	20020120	20020225	37	Rotated FRAME forecasts	3 h
December 2001+	20011210	20020104	26	Regular 1.0° analyses	6 h
December 1999+	19991120	19991231	42	Regular 1.5° analyses and 6 h forecasts	6 h

## 2.1. Domains

The operational DMI-HIRLAM model domains are shown in Figure 3. All domains are defined on a rotated grid with polar coordinates  $(P_{\text{lat}}, P_{\text{lon}}) = (0^\circ, 80^\circ)$ . The starting coordinates (southwest corner) in the rotated coordinate system and model resolution are as follows:



	G	E	D	N
$x_{lon,1}$	$-63.725^\circ$	$-54.275^\circ$	$-36.675^\circ$	$-29.075^\circ$
$y_{lat,1}$	$-37.527^\circ$	$-28.677^\circ$	$-15.177^\circ$	$-5.277^\circ$
dlat	$0.45^\circ$	$0.15^\circ$	$0.05^\circ$	$0.15^\circ$
dlon	$0.45^\circ$	$0.15^\circ$	$0.05^\circ$	$0.15^\circ$

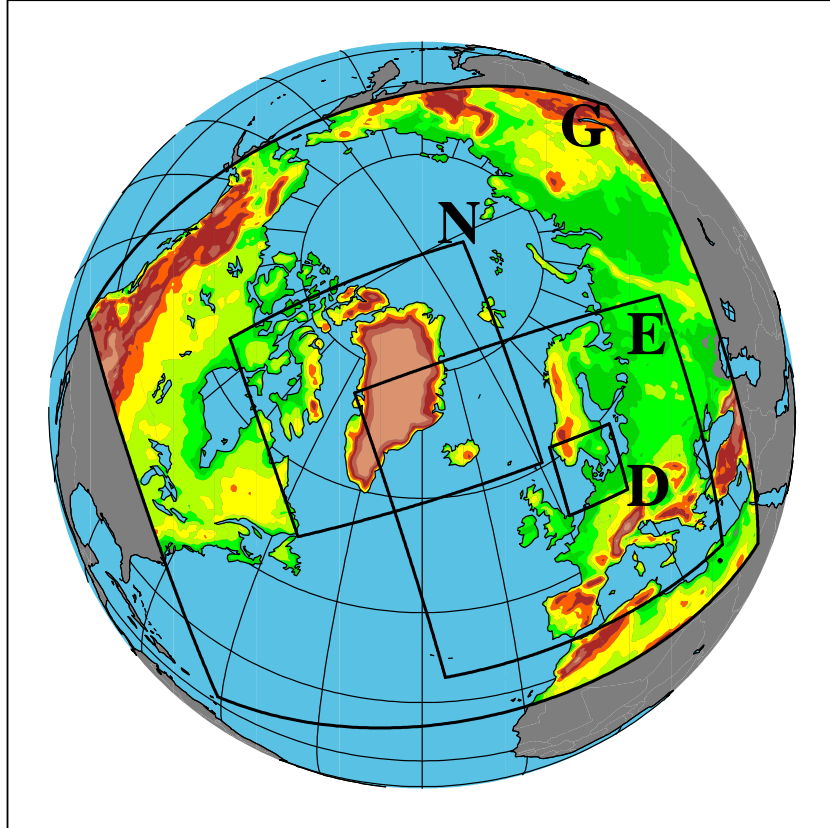


**Figure 3:** Operational DMI-HIRLAM areas.

## 2.2. Forecast model and boundary files

The model grid is a rotated, regular lat.-lon. Arakawa C grid with 40 (31) levels in the atmosphere and two layers in the soil. Prognostic variables at the lower boundary of the model, i.e. the sea surface and the bottom surface of the deepest soil layer, are kept constant during a forecast. The advection is Eulerian and second order accurate in space and time. To allow for longer time steps gravity wave terms are treated semi-implicitly. A computationally cheap radiation scheme (Savijärvi, 1990; Sass *et al.*, 1994), permitting calculation of radiation tendencies every physics time step, is applied.

Sub-grid scale physical processes (turbulence, convection, condensation, evaporation and cloud micro-physics) are parameterized. Only vertical sub-grid scale turbulent exchange is

considered. Linear fourth order (implicit/explicit) horizontal diffusion takes care of horizontal (i.e. along model coordinate surfaces) exchanges. It is applied mainly for numerical reasons, to prevent piling up of energy on the smallest resolved scales as a result of the energy cascade towards smaller scales. The cascade occurs because of the nonlinearity of the governing equations.

The parameterization of turbulence is based on the prognostic equation for turbulent kinetic energy (TKE). The vertical exchange coefficients depend on TKE and a stratification dependent mixing length. The scheme is ‘dry’ in the sense that vertical turbulent transports of  $q$ , specific humidity and  $q_c$ , cloud water, are calculated instead of transport calculations of the ‘moist’ variables  $\theta_L$ , liquid water potential temperature, and  $q_{tot} = q + q_c$ .

Parameterization of convection and condensation (both involving parameterization of cloud micro-physics) is done by the STRACO (Soft TRAnSition COnDensation) scheme. STRACO applies probability density functions for  $q_{tot} = q + q_c$ . The convective part applies a moisture convergence closure (Kuo, 1974), and the micro-physics related to the condensation and precipitation processes follow rather closely the comprehensive treatment by Sundqvist, 1993.

Surface layer similarity theory is used to calculate the turbulent fluxes of momentum, sensible heat and moisture at the surface. The fluxes are calculated for fractions of sea, ice and land. Budget equations (including molecular diffusion equations for the soil layers) are used to calculate the prognostic surface and ‘in soil’ variables over fraction of ice and land.

A more detailed documentation of the forecasting system at DMI is given in Sass *et al.*, 2002.

The lateral boundary values are provided by ECMWF. For the June/July 2002 and January/February 2002 periods (see Table 2) the so-called ECMWF FRAME boundary files were available and they were used as in the operational suite with 6 h old boundaries and updates for every 3 h for DMI-HIRLAM-G. For the December 2001+ period analyses files from ECMWF in a regular  $1^\circ \times 1^\circ$  grid from the 4 major SYNOP hours 00 UTC, 06 UTC, 12 UTC and 18 UTC were used with updates every 6 h for DMI-HIRLAM-G. For the last period, December 1999+, either analyses (valid at 00 UTC and 12 UTC) or 6 h forecasts (valid at 06 UTC and 18 UTC) ECMWF fields in a regular  $1.5^\circ \times 1.5^\circ$  grid were used as boundaries with updates every 6 h for DMI-HIRLAM-G.

### 2.3. Observation types used

In the old set-up the following observation types were used (in HIRVDA version 5.0.4, see Gustafsson *et al.*, 2001; Lindskog *et al.*, 2001; Sass *et al.*, 2002): SYNOP (surface pressure), SHIPS (surface pressure), DRIBU (surface pressure), PILOT (wind at all levels), TEMP (wind, temperature and humidity at all levels) and AIREP (wind and temperature; includes AMDAR and ACARS). For SYNOP, SHIPS and DRIBU reports, the station level height, multiplied by the gravitational acceleration, is utilised as a geopotential height observation at the observed station level pressure. In the new set-up the same observation types are used (in HIRVDA version 5.1.2) but in addition NOAA16 AMSU-A data from channels 1-10 (effectively only channels 5-10 since the observation errors have been set to a large value for channels 1-4) is included.

In general a few more upper air data are used in the new set-up due to the higher vertical

resolution. The fit to observations is somewhat better in the new set-up as found from the minimization of the observation cost function  $J_o$ , measuring the distance between the analysis and the observations. As an example, averaged values of the used number of different types of observations as well as  $J_o$  are given in Table 3 for the January/February 2002 period. The

**Table 3:** Averaged (final) values in the January/February 2002 period of number ( $N_{xx}$ ) of observations used and observation cost value (NOAA16 AMSU-A data *not* included) in the analyses for the given analyses hour, HH.  $N_{uv}$  is wind data from TEMPs, AIREPs and PILOTs;  $N_T$  is temperature data from TEMPs and AIREPs;  $N_q$  is humidity data from TEMPs; and  $N_Z$  is surface pressure data from SYNOPs, SHIPs and DRIBUs (buoys). D1A is DMI-HIRLAM-E, D1C is DMI-HIRLAM-E-new, G4A is DMI-HIRLAM-G and G4C is DMI-HIRLAM-G-new.

HH		$N_{uv}$	$N_T$	$N_q$	$N_Z$	$J_o$		$N_{uv}$	$N_T$	$N_q$	$N_Z$	$J_o$
0	D1A	3605	3300	2530	1271	6926.92	G4A	6352	7398	5928	2224	11413.01
0	D1C	3625	3315	2582	1269	6248.63	G4C	6379	7451	5966	2214	10664.44
12	D1A	3433	3147	2310	1434	6440.63	G4A	5922	6972	5600	2383	10782.33
12	D1C	3460	3165	2360	1431	5887.63	G4C	5961	7031	5642	2371	10143.45
6	D1A	1464	1317	925	1441	2713.89	G4A	1847	1655	951	2410	2975.25
6	D1C	1469	1321	950	1437	2465.24	G4C	1853	1661	956	2398	2823.32
18	D1A	1477	1249	799	1454	2575.58	G4A	2202	1954	841	2472	3155.39
18	D1C	1484	1253	827	1449	2318.46	G4C	2206	1960	845	2457	2966.29
3	D1A	77	67	32	1272	385.28	G4A	454	442	34	1758	738.03
3	D1C	77	67	34	1269	356.49	G4C	454	443	34	1751	702.41
9	D1A	135	131	3	1367	401.50	G4A	223	218	3	1855	564.56
9	D1C	135	131	3	1365	385.70	G4C	223	218	3	1848	544.07
15	D1A	199	195	3	1361	449.26	G4A	563	559	9	1893	817.24
15	D1C	199	196	3	1359	438.95	G4C	563	559	9	1885	793.78
21	D1A	119	119	0	1261	342.69	G4A	487	489	7	1762	689.24
21	D1C	119	118	0	1258	327.19	G4C	487	489	7	1754	655.98

$J_o$  values listed in the table for the new versions exclude the part from NOAA16 AMSU-A data so the values are comparable. It can be concluded that the use of the satellite data do not make the fit to the upper level data worse – at least not as much as any benefit from increasing the number of vertical levels from 31 to 40. The number of surface pressure data used is reduced marginally in the new setup. It might be extra rejections of bad SHIPs or DRIBUs by use of information from the satellite data but that is speculations so far.

## 2.4. Mike21

The storm surge model, Mike21, has been run as in the operational environment (see Nielsen, 2001 for details). The model is forced by the HIRLAM surface level pressure and stressed 10 m wind fields (i.e. 10 m winds that gives the HIRLAM surface stress with the drag formula used in Mike21) from the DMI-HIRLAM-E model. It is run up to 54 h and a new run is made every 6th hour corresponding to a new HIRLAM analysis and forecast. The first run in a given test period is started from initial fields from the Mike21 tape archive. No analysis take place. Subsequent Mike21 runs in the test period are started from the new initial fields produced by the test run. The 5 cases studied are listed in Table 4. The results from these runs are

**Table 4:** Cases studied with the storm surge model Mike21.

	period	type
Case I	20011217-20011221	high water in the Baltic Sea December 20th
Case II	20011230-20020103	high water in the Baltic Sea January 2nd
Case III	20020125-20020130	storm surge in the Jutland Wadden Sea January 28th
Case IV	20020218-20020224	high water in the Baltic Sea February 21st and subsequent storm surge in the Jutland Wadden Sea February 22nd and 23rd
Case V	19991201-19991205	Danish Storm December 1999

given by the peak value of a given forecast within a time interval of some hours around the time of the observed maximum water level at the given place. Thus, a phase error of a given Mike21 forecast is not taken into account and a “worse” HIRLAM forecast might actually give a better result in the storm surge model, since the exact time of the maximum is not as critical as the peak value.

### 3. Results

We analyse model scores in two ways: a) observation verification (obs-verification), where model forecasts are verified against observations, and b) field verification, where model forecasts are compared with their own verifying analyses on a grid point by grid point basis.

#### 3.1. Parallel runs

Obs-verification results for the EWGLAM station list for the combination of the four periods are shown in Figures 4 and 5. The DMI-HIRLAM-E-new (D1C) has clearly better rms-scores (root mean square scores) than DMI-HIRLAM-E (D1A) for mslp, 2mT, geopotential height at 850 hPa, 500 hPa and 250 hPa and temperature and wind at 250 hPa. For the other parameters the rms-scores are very close.

Obs-verification results using a Danish station list for the combination of the four periods are shown in Figure 6. In general, the differences in rms-scores are rather small but differences in bias-scores are somewhat larger, in particular for 2mT biases. For mslp DMI-HIRLAM-G-new has better rms-scores than DMI-HIRLAM-G. For 2mT DMI-HIRLAM-G has better rms-scores than DMI-HIRLAM-G-new, DMI-HIRLAM-E-new has better rms-scores compared to DMI-HIRLAM-E for forecast lengths shorter than 36 h and worse rms-scores for forecast lengths longer than 36 h, and DMI-HIRLAM-D-new has somewhat better rms-scores than DMI-HIRLAM-D but worse bias-scores. DMI-HIRLAM-E-new has worse 2mT bias-scores than DMI-HIRLAM-E. For 10mW DMI-HIRLAM-D-new has better bias-scores than DMI-HIRLAM-D, otherwise the differences are small. DMI-HIRLAM-E has a little better rms-scores and bias-scores than DMI-HIRLAM-E-new except for the longest forecast lengths.

Obs-verification results using a Greenland station list for the combination of the four periods are shown in Figures 7 and 8. The largest differences in scores for the Greenland

station list for DMI-HIRLAM-G and DMI-HIRLAM-G-new occur for mslp for which DMI-HIRLAM-G has the better scores. The scores for DMI-HIRLAM-N and DMI-HIRLAM-N-new are close except for DMI-HIRLAM-N-new having general better scores for temperature at 2 m and the upper levels shown in Figure 8.

Obs-verification of the vertical structure of temperature and geopotential height is illustrated in Figures 9 and 10. Figure 9 shows bias scores of temperature at analysis time and for the 12, 24 and 36 hour forecasts of DMI-HIRLAM-E and DMI-HIRLAM-E-new as a function of pressure in the January/February 2002 period (bottom) and in the June/July 2002 period. The vertical structure of temperature is much better in the new set-up both in the summer period and in the winter period. Figure 10 shows rms-scores for DMI-HIRLAM-E-new and differences in rms scores between DMI-HIRLAM-E and DMI-HIRLAM-E-new at analysis time and for the 12, 24 and 36 hour forecasts as a function of pressure in the January/February 2002 period. Here, the tendency from the bias plots in Figure 9 shows up again with DMI-HIRLAM-E-new having the better scores. The same tendencies are seen for the June/July 2002 period.

The relative humidity is illustrated in Figure 11 that shows observed and forecasted relative humidity averaged over the June/July period for a number of Danish SYNOP stations reporting (at least) hourly. The model versions in the new set-up fit much better to the observed values, in particular for the land stations. All model versions give quite reasonable phases of the diurnal cycle with a minimum around 14 UTC and a maximum at night around 03 UTC. The amplitude of the diurnal variation is very good for the land stations and a little bit too small for the coastal stations.

Standard verification of precipitation in terms of contingency tables for the considered periods has been done. Tables 5-12 show the results for a summer period (June/July 2002) and a winter period (January/February 2002). These periods were chosen since the coupling to ECMWF boundaries are equivalent to the operational usage for these runs.

The numbers in the contingency tables are obtained by counting the number of observed and predicted precipitation amounts in each of five classes for the SYNOP stations. The five precipitation classes are (precipitation amounts in mm):  $P1 < 0.2$ ,  $0.2 \leq P2 < 1.0$ ,  $1.0 \leq P3 < 5$ ,  $5 \leq P4 < 10$  and  $P5 \geq 10$ .  $P$  is either F (forecast) or O (observation) in the given tables. The “sum” rows and columns are the sums of the numbers in the given observation classes or forecast classes, respectively. The %FO/sum entries in the tables are the percentage of elements in the diagonal. For the contingency tables using the Danish station list, the results corresponding to the “resultatkontrakt” are given. These numbers corresponds to the %FO/sum entries for a contingency table with three classes (limits in mm:  $P < 0.3$ ,  $0.3 \leq P < 5$  and  $P \geq 5$ ).

Note that the observed values are uncorrected values. Thus, small observed precipitation values are most likely underestimated.

The verification is done on the national scale against the Danish SYNOP station list and on the European scale against the EWGLAM (European Working Group on Limited Area Model) station list. The Danish SYNOP station list includes the following stations (when available): 6030, 6041, 6052, 6058, 6060, 6070, 6079, 6080, 6081, 6104, 6110, 6111, 6119, 6120, 6156, 6160, 6170, 6180, 6181, 6190. See Figure 12 for the position of these stations.

Tables 5-6 for the June/July 2002 period show contingency tables of accumulated precipitation over 12 hours based on the national station list for the three model versions covering Denmark, and Tables 7-8 show contingency tables of accumulated precipitation over 12 hours based on the EWGLAM station list for the “G” and “E” models. For the January/February 2002 period Tables 9-10 show contingency tables of accumulated precipitation over 12 hours based on the national station list and Tables 11-12 show contingency tables of accumulated precipitation over 12 hours based on the EWGLAM station list.

Tables 5, 7, 9 and 11 show results for 12 hour accumulated precipitation starting at 6 hour forecast length, and Tables 6, 8, 10 and 12 show results for 12 hour accumulated precipitation starting at 18 hour forecast length.

In general the old model versions have better overall scores based on a better prediction of the O1 class. The new model versions have better predictions of the O5 class in the June/July 2002 period and also in the January/February 2002 period for the EWGLAM stations. For the June/July 2002 period the better prediction of the O1 class for the old model versions compared to the new model versions are linked to higher numbers in the upper right corners of the tables. Similarly, the better prediction of the O5 class by the new model version is linked to higher numbers in the lower left corners of the tables compared to the old model versions.

### 3.2. Field verification

Since the stations involved in the standard obs-verifications cover a limited part of the model domains, the forecasts are also compared with (initialized) analyses from their own data assimilation suite valid at the same time as the forecasts (field-verification). Thus, information on data sparse areas is available. It should, however, be remarked that not too much should be read into these results since the (initialized) analyses are not the full truth and they depend on the model itself.

The field verification study shows that the new model versions tend to improve over the old model versions but not in all respects.

Averaged (over the full model area) bias and rms scores for mslp, T850 (850 hPa temperature) and H500 (geopotential height) are shown in Table 13. The difference between versions is considered “significant” if the averaged results differ by more than 2.5 Pa (mslp), 2 gpm (H500) and 0.02 K (T850), respectively.

For mslp, the better version with respect to bias scores varies from period to period. For rms scores DMI-HIRLAM-G and DMI-HIRLAM-G-new have similar scores whereas DMI-HIRLAM-E-new has better scores than DMI-HIRLAM-E.

For 500 hPa geopotential height (H500) the new versions in general have better rms scores than the old versions. With respect to H500 bias scores DMI-HIRLAM-G has better scores than DMI-HIRLAM-G-new for the longer forecast lengths (48 h and 36 h) and vice versa for the shorter forecast lengths (12 h and 24 h). DMI-HIRLAM-E-new has in general (except for 48 h in the December 2001+ and December 1999+ periods) better bias scores than DMI-HIRLAM-E.

The behavior for temperature at 850 hPa is somewhat different. DMI-HIRLAM-G has better bias as well as rms scores than DMI-HIRLAM-G-new in all periods. DMI-HIRLAM-E-new has better bias scores in the January/February 2002 and December 1999+ periods

**Table 5:** 12 h accumulated precipitation: Contingency tables for the 20020610-20020712 period for 6 to 18 hour forecasts. Danish station list. F stands for forecast and O for observation. The number is the class number (see text). %FO is the percentage of the forecasted values in the same class as the observation class. The number in the parenthesis in the head of the subtables is the corresponding number (%FO/sum entry) for the “resultatkontrakt” (see text).

G4A 0206/0207 (67.5 %)							G4C 0206/0207 (62.1 %)						
$\frac{\text{obs} \rightarrow}{\downarrow \text{for}}$	O1	O2	O3	O4	O5	sum	$\frac{\text{obs} \rightarrow}{\downarrow \text{for}}$	O1	O2	O3	O4	O5	sum
F1	<b>421</b>	42	32	10	0	505	F1	<b>350</b>	36	21	8	0	415
F2	139	<b>53</b>	75	17	14	298	F2	181	<b>44</b>	47	15	8	295
F3	41	56	<b>113</b>	58	27	295	F3	68	58	<b>128</b>	44	22	320
F4	3	1	8	<b>21</b>	14	47	F4	6	14	28	<b>23</b>	20	91
F5	1	0	3	1	<b>14</b>	19	F5	0	0	7	17	<b>19</b>	43
sum	605	152	231	107	69	1164	sum	605	152	231	107	69	1164
%FO	70	35	49	20	20	53	%FO	58	29	55	21	28	48

D1A 0206/0207 (66.3 %)							D1C 0206/0207 (57.5 %)						
$\frac{\text{obs} \rightarrow}{\downarrow \text{for}}$	O1	O2	O3	O4	O5	sum	$\frac{\text{obs} \rightarrow}{\downarrow \text{for}}$	O1	O2	O3	O4	O5	sum
F1	<b>363</b>	28	17	3	0	411	F1	<b>270</b>	24	14	0	0	308
F2	185	<b>62</b>	60	16	10	333	F2	206	<b>33</b>	28	8	2	277
F3	53	56	<b>133</b>	59	28	329	F3	118	81	<b>135</b>	51	24	409
F4	3	6	17	<b>21</b>	15	62	F4	9	12	44	<b>39</b>	14	118
F5	1	0	4	8	<b>16</b>	29	F5	2	2	10	9	<b>29</b>	52
sum	605	152	231	107	69	1164	sum	605	152	231	107	69	1164
%FO	60	41	58	20	23	51	%FO	45	22	58	36	42	43

D0A 0206/0207 (68.5 %)							D0C 0206/0207 (54.9 %)						
$\frac{\text{obs} \rightarrow}{\downarrow \text{for}}$	O1	O2	O3	O4	O5	sum	$\frac{\text{obs} \rightarrow}{\downarrow \text{for}}$	O1	O2	O3	O4	O5	sum
F1	<b>435</b>	43	36	10	5	529	F1	<b>250</b>	17	9	1	0	277
F2	133	<b>59</b>	63	23	12	290	F2	183	<b>33</b>	24	6	3	249
F3	36	45	<b>113</b>	45	24	263	F3	148	78	<b>124</b>	42	16	408
F4	1	5	14	<b>21</b>	8	49	F4	19	20	60	<b>36</b>	19	154
F5	0	0	5	8	<b>20</b>	33	F5	5	4	14	22	<b>31</b>	76
sum	605	152	231	107	69	1164	sum	605	152	231	107	69	1164
%FO	72	39	49	20	29	56	%FO	41	22	54	34	45	41

**Table 6:** 12 h accumulated precipitation: Contingency tables for the 20020610-20020712 period for 18 to 30 hour forecasts. Danish station list. F stands for forecast and O for observation. The number is the class number (see text). %FO is the percentage of the forecasted values in the same class as the observation class. The number in the parenthesis in the head of the subtables is the corresponding number (%FO/sum entry) for the “resultatkontrakt”.

G4A 0206/0207 (65.2%)							G4C 0206/0207 (56.8%)						
$\frac{\text{obs} \rightarrow}{\downarrow \text{for}}$	O1	O2	O3	O4	O5	sum	$\frac{\text{obs} \rightarrow}{\downarrow \text{for}}$	O1	O2	O3	O4	O5	sum
F1	<b>387</b>	48	23	8	3	469	F1	<b>280</b>	41	14	10	2	347
F2	159	<b>47</b>	75	21	11	313	F2	217	<b>41</b>	57	23	11	349
F3	60	58	<b>115</b>	54	21	308	F3	101	65	<b>127</b>	38	23	354
F4	2	3	15	<b>16</b>	12	48	F4	9	8	24	<b>27</b>	11	79
F5	0	0	5	4	<b>17</b>	26	F5	1	1	11	5	<b>17</b>	35
sum	608	156	233	103	64	1164	sum	608	156	233	103	64	1164
%FO	64	30	49	16	27	50	%FO	46	26	55	26	27	42

D1A 0206/0207 (62.9%)							D1C 0206/0207 (54.5%)						
$\frac{\text{obs} \rightarrow}{\downarrow \text{for}}$	O1	O2	O3	O4	O5	sum	$\frac{\text{obs} \rightarrow}{\downarrow \text{for}}$	O1	O2	O3	O4	O5	sum
F1	<b>339</b>	46	21	8	2	416	F1	<b>244</b>	22	11	2	1	280
F2	193	<b>36</b>	55	12	7	303	F2	224	<b>43</b>	43	15	5	330
F3	74	71	<b>133</b>	49	22	349	F3	127	71	<b>129</b>	42	22	391
F4	2	3	19	<b>26</b>	19	69	F4	11	19	38	<b>29</b>	18	115
F5	0	0	5	8	<b>14</b>	27	F5	2	1	12	15	<b>18</b>	48
sum	608	156	233	103	64	1164	sum	608	156	233	103	64	1164
%FO	56	23	57	25	22	47	%FO	40	28	55	28	28	40

D0A 0206/0207 (65.4%)							D0C 0206/0207 (49.9%)						
$\frac{\text{obs} \rightarrow}{\downarrow \text{for}}$	O1	O2	O3	O4	O5	sum	$\frac{\text{obs} \rightarrow}{\downarrow \text{for}}$	O1	O2	O3	O4	O5	sum
F1	<b>373</b>	51	30	8	6	468	F1	<b>224</b>	12	12	4	0	252
F2	179	44	71	22	6	322	F2	192	47	29	11	3	282
F3	53	58	<b>110</b>	41	21	283	F3	159	67	<b>99</b>	37	15	377
F4	3	3	15	<b>20</b>	16	57	F4	23	22	64	<b>28</b>	23	160
F5	0	0	7	12	<b>15</b>	34	F5	10	8	29	23	<b>23</b>	93
sum	608	156	233	103	64	1164	sum	608	156	233	103	64	1164
%FO	61	28	47	19	23	48	%FO	37	30	42	27	36	36



**Table 7:** 12 h accumulated precipitation: Contingency tables for the 20020610-20020712 period for 6 to 18 hour forecasts. EWGLAM station list. F stands for forecast and O for observation. The number is the class number (see text). %FO is the percentage of the forecasted values in the same class as the observation class.

G4A 0206/0207							G4C 0206/0207						
$\frac{\text{obs} \rightarrow}{\downarrow \text{for}}$	O1	O2	O3	O4	O5	sum	$\frac{\text{obs} \rightarrow}{\downarrow \text{for}}$	O1	O2	O3	O4	O5	sum
F1	<b>12769</b>	644	409	99	<b>70</b>	13991	F1	<b>12398</b>	562	356	86	<b>55</b>	13457
F2	1764	<b>656</b>	689	194	94	3397	F2	1881	<b>539</b>	453	131	66	3070
F3	574	356	<b>655</b>	325	212	2122	F3	791	522	<b>816</b>	308	166	2603
F4	42	22	100	<b>93</b>	111	368	F4	66	45	186	<b>153</b>	120	570
F5	5	0	14	24	<b>65</b>	108	F5	18	10	56	57	<b>145</b>	286
sum	15154	1678	1867	735	552	19986	sum	15154	1678	1867	735	552	19986
%FO	84	39	35	13	12	71	%FO	82	32	44	21	26	70

D1A 0206/0207							D1C 0206/0207						
$\frac{\text{obs} \rightarrow}{\downarrow \text{for}}$	O1	O2	O3	O4	O5	sum	$\frac{\text{obs} \rightarrow}{\downarrow \text{for}}$	O1	O2	O3	O4	O5	sum
F1	<b>12769</b>	610	368	82	<b>69</b>	13898	F1	<b>11562</b>	446	261	68	<b>52</b>	12389
F2	1760	<b>620</b>	582	152	82	3196	F2	2092	<b>476</b>	376	87	49	3080
F3	581	417	<b>775</b>	361	211	2345	F3	1259	609	<b>862</b>	293	127	3150
F4	36	29	122	<b>106</b>	123	416	F4	173	108	276	<b>187</b>	137	881
F5	8	2	20	34	<b>67</b>	131	F5	68	39	92	100	<b>187</b>	486
sum	15154	1678	1867	735	552	19986	sum	15154	1678	1867	735	552	19986
%FO	84	37	42	14	12	72	%FO	76	28	46	25	34	66

**Table 8:** 12 h accumulated precipitation: Contingency tables for the 20020610-20020712 period for 18 to 30 hour forecasts. EWGLAM station list. F stands for forecast and O for observation. The number is the class number (see text). %FO is the percentage of the forecasted values in the same class as the observation class.

G4A 0206/0207							G4C 0206/0207						
$\frac{\text{obs} \rightarrow}{\downarrow \text{for}}$	O1	O2	O3	O4	O5	sum	$\frac{\text{obs} \rightarrow}{\downarrow \text{for}}$	O1	O2	O3	O4	O5	sum
F1	<b>12554</b>	626	399	101	<b>74</b>	13754	F1	<b>12154</b>	507	352	90	<b>66</b>	13169
F2	1948	<b>626</b>	665	181	104	3524	F2	2012	<b>526</b>	474	130	72	3214
F3	642	373	<b>648</b>	322	238	2223	F3	927	542	<b>776</b>	320	189	2754
F4	48	32	111	<b>91</b>	80	362	F4	80	64	191	<b>134</b>	102	571
F5	9	4	28	31	<b>49</b>	121	F5	28	22	58	52	<b>116</b>	276
sum	15201	1661	1851	726	545	19984	sum	15201	1661	1851	726	545	19984
%FO	83	38	35	13	9	70	%FO	80	32	42	18	21	69

D1A 0206/0207							D1C 0206/0207						
$\frac{\text{obs} \rightarrow}{\downarrow \text{for}}$	O1	O2	O3	O4	O5	sum	$\frac{\text{obs} \rightarrow}{\downarrow \text{for}}$	O1	O2	O3	O4	O5	sum
F1	<b>12733</b>	594	423	102	<b>86</b>	13938	F1	<b>11546</b>	468	296	80	<b>63</b>	12453
F2	1771	<b>606</b>	569	156	90	3192	F2	2072	<b>463</b>	382	80	61	3058
F3	637	425	<b>719</b>	336	211	2328	F3	1302	562	<b>841</b>	296	173	3174
F4	48	31	119	<b>104</b>	100	402	F4	196	123	259	<b>181</b>	116	875
F5	12	5	21	28	<b>58</b>	124	F5	85	45	73	89	<b>132</b>	424
sum	15201	1661	1851	726	545	19984	sum	15201	1661	1851	726	545	19984
%FO	84	36	39	14	11	71	%FO	76	28	45	25	24	66

**Table 9:** 12 h accumulated precipitation: Contingency tables for the 20020120-20020225 period for 6 to 18 hour forecasts. Danish station list. F stands for forecast and O for observation. The number is the class number (see text). %FO is the percentage of the forecasted values in the same class as the observation class. The number in the parenthesis in the head of the subtables is the corresponding number (%FO/sum entry) for the “resultatkontrakt”.

G4A 0201/0202 (69.1 %)							G4C 0201/0202 (65.5 %)						
$\frac{\text{obs} \rightarrow}{\downarrow \text{for}}$	O1	O2	O3	O4	O5	sum	$\frac{\text{obs} \rightarrow}{\downarrow \text{for}}$	O1	O2	O3	O4	O5	sum
F1	<b>321</b>	23	2	0	0	346	F1	<b>290</b>	16	3	0	0	309
F2	171	<b>118</b>	95	7	0	391	F2	164	<b>77</b>	31	0	0	272
F3	28	95	<b>203</b>	82	9	417	F3	67	140	<b>221</b>	62	5	495
F4	2	11	59	<b>52</b>	13	137	F4	1	13	101	<b>73</b>	16	204
F5	0	0	5	11	<b>6</b>	22	F5	0	1	8	17	<b>7</b>	33
sum	522	247	364	152	28	1313	sum	522	247	364	152	28	1313
%FO	61	48	56	34	21	53	%FO	56	31	61	48	25	51
D1A 0201/0202 (69.4 %)							D1C 0201/0202 (65.8 %)						
$\frac{\text{obs} \rightarrow}{\downarrow \text{for}}$	O1	O2	O3	O4	O5	sum	$\frac{\text{obs} \rightarrow}{\downarrow \text{for}}$	O1	O2	O3	O4	O5	sum
F1	<b>301</b>	13	1	0	0	315	F1	<b>292</b>	9	3	1	0	305
F2	181	<b>103</b>	48	1	0	333	F2	164	<b>71</b>	28	0	0	263
F3	38	117	<b>228</b>	60	7	450	F3	64	149	<b>219</b>	58	9	499
F4	2	14	76	<b>75</b>	12	179	F4	2	17	102	<b>77</b>	12	210
F5	0	0	11	16	<b>9</b>	36	F5	0	1	12	16	<b>7</b>	36
sum	522	247	364	152	28	1313	sum	522	247	364	152	28	1313
%FO	58	42	63	49	32	55	%FO	56	29	60	51	25	51
D0A 0201/0202 (67.3 %)							D0C 0201/0202 (64.6 %)						
$\frac{\text{obs} \rightarrow}{\downarrow \text{for}}$	O1	O2	O3	O4	O5	sum	$\frac{\text{obs} \rightarrow}{\downarrow \text{for}}$	O1	O2	O3	O4	O5	sum
F1	<b>302</b>	11	4	0	0	317	F1	<b>278</b>	9	4	0	0	291
F2	179	<b>102</b>	41	1	0	323	F2	167	<b>66</b>	22	1	0	256
F3	38	118	<b>209</b>	53	5	423	F3	72	153	<b>219</b>	53	6	503
F4	3	16	93	<b>75</b>	13	200	F4	5	19	104	<b>78</b>	13	219
F5	0	0	17	23	<b>10</b>	50	F5	0	0	15	20	<b>9</b>	44
sum	522	247	364	152	28	1313	sum	522	247	364	152	28	1313
%FO	58	41	57	49	36	53	%FO	53	27	60	51	32	50

**Table 10:** 12h accumulated precipitation: Contingency tables for the 20020120-20020225 period for 18 to 30 hour forecasts. Danish station list. F stands for forecast and O for observation. The number is the class number (see text). %FO is the percentage of the forecasted values in the same class as the observation class. The number in the parenthesis in the head of the subtables is the corresponding number (%FO/sum entry) for the “resultatkontrakt”.

G4A 0201/0202 (64.9%)							G4C 0201/0202 (63.3%)						
$\frac{\text{obs} \rightarrow}{\downarrow \text{for}}$	O1	O2	O3	O4	O5	sum	$\frac{\text{obs} \rightarrow}{\downarrow \text{for}}$	O1	O2	O3	O4	O5	sum
F1	<b>285</b>	12	1	0	0	298	F1	<b>248</b>	13	6	1	0	268
F2	171	<b>97</b>	81	9	0	358	F2	162	<b>73</b>	49	2	0	286
F3	57	119	<b>180</b>	59	10	425	F3	107	145	<b>202</b>	56	5	515
F4	9	15	81	<b>80</b>	18	203	F4	5	15	80	<b>69</b>	15	184
F5	0	3	11	8	<b>7</b>	29	F5	0	0	17	<b>28</b>	15	60
sum	522	246	354	156	35	1313	sum	522	246	354	156	35	1313
%FO	55	39	51	51	20	49	%FO	48	30	57	44	43	46

D1A 0201/0202 (63.5%)							D1C 0201/0202 (61.4%)						
$\frac{\text{obs} \rightarrow}{\downarrow \text{for}}$	O1	O2	O3	O4	O5	sum	$\frac{\text{obs} \rightarrow}{\downarrow \text{for}}$	O1	O2	O3	O4	O5	sum
F1	<b>269</b>	11	6	0	0	286	F1	<b>262</b>	16	18	2	0	298
F2	174	<b>91</b>	66	10	0	341	F2	157	<b>55</b>	29	10	1	252
F3	66	122	<b>176</b>	48	10	422	F3	88	165	<b>222</b>	72	11	558
F4	10	22	94	<b>82</b>	12	220	F4	13	9	73	<b>49</b>	17	161
F5	<b>3</b>	0	12	16	<b>13</b>	44	F5	<b>2</b>	1	12	23	6	44
sum	522	246	354	156	35	1313	sum	522	246	354	156	35	1313
%FO	52	37	50	53	37	48	%FO	50	22	63	31	17	45

D0A 0201/0202 (63.1%)							D0C 0201/0202 (60.5%)						
$\frac{\text{obs} \rightarrow}{\downarrow \text{for}}$	O1	O2	O3	O4	O5	sum	$\frac{\text{obs} \rightarrow}{\downarrow \text{for}}$	O1	O2	O3	O4	O5	sum
F1	<b>273</b>	15	3	0	0	291	F1	<b>243</b>	15	15	0	0	273
F2	170	<b>85</b>	64	9	0	328	F2	167	<b>50</b>	29	9	2	257
F3	66	122	<b>166</b>	41	9	404	F3	97	165	<b>215</b>	64	10	551
F4	7	23	102	<b>82</b>	11	225	F4	13	15	80	<b>58</b>	13	179
F5	<b>6</b>	1	19	24	<b>15</b>	65	F5	<b>2</b>	1	15	25	10	53
sum	522	246	354	156	35	1313	sum	522	246	354	156	35	1313
%FO	52	35	47	53	43	47	%FO	47	20	61	37	29	44

**Table 11:** 12h accumulated precipitation: Contingency tables for the 20020120-20020225 period for 6 to 18 hour forecasts. EWGLAM station list. F stands for forecast and O for observation. The number is the class number (see text). %FO is the percentage of the forecasted values in the same class as the observation class.

G4A 0201/0202							G4C 0201/0202						
$\frac{\text{obs} \rightarrow}{\downarrow \text{for}}$	O1	O2	O3	O4	O5	sum	$\frac{\text{obs} \rightarrow}{\downarrow \text{for}}$	O1	O2	O3	O4	O5	sum
F1	<b>9382</b>	326	123	9	7	9847	F1	<b>9326</b>	265	74	11	4	9680
F2	3467	<b>1284</b>	852	96	27	5726	F2	3349	<b>1042</b>	539	47	21	4998
F3	1248	1112	<b>2229</b>	615	171	5375	F3	1434	1369	<b>2364</b>	498	125	5790
F4	83	74	359	<b>384</b>	202	1102	F4	71	117	545	<b>486</b>	190	1409
F5	<b>10</b>	13	56	79	<b>135</b>	293	F5	<b>10</b>	16	97	141	<b>202</b>	466
sum	14190	2809	3619	1183	542	22343	sum	14190	2809	3619	1183	542	22343
%FO	66	46	62	32	25	60	%FO	66	37	65	41	37	60

D1A 0201/0202							D1C 0201/0202						
$\frac{\text{obs} \rightarrow}{\downarrow \text{for}}$	O1	O2	O3	O4	O5	sum	$\frac{\text{obs} \rightarrow}{\downarrow \text{for}}$	O1	O2	O3	O4	O5	sum
F1	<b>9516</b>	340	110	24	16	10006	F1	<b>9278</b>	301	105	31	14	9729
F2	3137	<b>1118</b>	688	65	11	5019	F2	3235	<b>946</b>	459	41	21	4702
F3	1426	1220	<b>2275</b>	540	146	5607	F3	1550	1411	<b>2377</b>	454	100	5892
F4	98	114	475	<b>452</b>	212	1351	F4	106	130	580	<b>501</b>	197	1514
F5	<b>13</b>	17	71	102	<b>157</b>	360	F5	<b>21</b>	21	98	156	<b>210</b>	506
sum	14190	2809	3619	1183	542	22343	sum	14190	2809	3619	1183	542	22343
%FO	67	40	63	38	29	61	%FO	65	34	66	42	39	60

**Table 12:** 12h accumulated precipitation: Contingency tables for the 20020120-20020225 period for 18 to 30 hour forecasts. EWGLAM station list. F stands for forecast and O for observation. The number is the class number (see text). %FO is the percentage of the forecasted values in the same class as the observation class.

G4A 0201/0202							G4C 0201/0202						
$\frac{\text{obs} \rightarrow}{\downarrow \text{for}}$	O1	O2	O3	O4	O5	sum	$\frac{\text{obs} \rightarrow}{\downarrow \text{for}}$	O1	O2	O3	O4	O5	sum
F1	<b>8966</b>	281	92	11	5	9355	F1	<b>8855</b>	251	97	13	10	9226
F2	3562	<b>1126</b>	816	122	46	5672	F2	3590	<b>930</b>	525	67	41	5153
F3	1531	1231	<b>2256</b>	617	176	5811	F3	1632	1422	<b>2358</b>	542	134	6088
F4	117	109	389	<b>380</b>	225	1220	F4	101	134	545	<b>467</b>	214	1461
F5	<b>19</b>	19	69	82	<b>94</b>	283	F5	<b>17</b>	29	97	123	<b>147</b>	413
sum	14195	2766	3622	1212	546	22341	sum	14195	2766	3622	1212	546	22341
%FO	63	41	62	31	17	57	%FO	62	34	65	39	27	57

D1A 0201/0202							D1C 0201/0202						
$\frac{\text{obs} \rightarrow}{\downarrow \text{for}}$	O1	O2	O3	O4	O5	sum	$\frac{\text{obs} \rightarrow}{\downarrow \text{for}}$	O1	O2	O3	O4	O5	sum
F1	<b>9382</b>	343	152	27	17	9921	F1	<b>9155</b>	334	154	32	21	9696
F2	3088	<b>997</b>	685	93	36	4899	F2	3304	<b>914</b>	558	62	28	4866
F3	1577	1290	<b>2243</b>	582	173	5865	F3	1593	1352	<b>2285</b>	526	128	5884
F4	121	114	461	<b>408</b>	202	1306	F4	118	142	532	<b>460</b>	192	1444
F5	<b>27</b>	22	81	102	<b>118</b>	350	F5	<b>25</b>	24	93	132	<b>177</b>	451
sum	14195	2766	3622	1212	546	22341	sum	14195	2766	3622	1212	546	22341
%FO	66	36	62	34	22	59	%FO	64	33	63	38	32	58

**Table 13:** Field verification results for mslp (in hPa), 850 hPa temperature (T850) in K and 500 hPa geopotential height (H500) in gpm. For a given variable and forecast length, the better model has the result in a bold font if the difference is “significant”.

type	FCL	yymm	DMI-HIRLAM-G				DMI-HIRLAM-E			
			old		new		old		new	
			bias	rms	bias	rms	bias	rms	bias	rms
mslp	12	0201	-0.12	1.26	<b>-0.08</b>	1.24	-0.29	1.41	<b>-0.22</b>	<b>1.35</b>
mslp	24	0201	-0.14	1.84	<b>-0.06</b>	<b>1.81</b>	-0.45	2.07	<b>-0.34</b>	<b>1.99</b>
mslp	36	0201	-0.15	2.43	<b>-0.03</b>	<b>2.40</b>	-0.54	2.79	<b>-0.37</b>	<b>2.69</b>
mslp	48	0201	-0.24	3.03	<b>-0.09</b>	3.01	-0.66	3.54	<b>-0.42</b>	<b>3.47</b>
mslp	12	0206	<b>0.00</b>	0.95	0.04	0.93	0.04	1.00	0.06	<b>0.94</b>
mslp	24	0206	<b>0.15</b>	1.32	0.22	1.30	<b>0.14</b>	1.29	0.17	<b>1.22</b>
mslp	36	0206	<b>0.22</b>	1.74	0.33	1.73	<b>0.15</b>	1.76	0.18	<b>1.64</b>
mslp	48	0206	<b>0.29</b>	2.14	0.41	2.13	0.31	2.20	<b>0.27</b>	<b>2.03</b>
mslp	12	0112	<b>-0.02</b>	1.29	0.09	1.30	-0.06	1.23	0.05	1.24
mslp	24	0112	<b>0.05</b>	1.79	0.20	1.81	<b>-0.03</b>	<b>1.79</b>	0.11	1.82
mslp	36	0112	<b>0.07</b>	2.24	0.28	2.25	<b>-0.07</b>	2.35	0.15	2.36
mslp	48	0112	<b>0.09</b>	2.70	0.34	2.70	<b>-0.09</b>	3.00	0.23	2.99
mslp	12	9912	-0.07	1.71	0.05	1.72	-0.04	1.48	0.05	<b>1.43</b>
mslp	24	9912	-0.14	2.28	<b>0.06</b>	2.27	-0.23	2.20	<b>-0.11</b>	<b>2.12</b>
mslp	36	9912	-0.18	2.77	<b>0.08</b>	<b>2.73</b>	-0.39	2.93	<b>-0.25</b>	<b>2.81</b>
mslp	48	9912	-0.24	3.27	<b>0.08</b>	<b>3.21</b>	-0.54	3.76	<b>-0.37</b>	<b>3.56</b>
H500	12	0201	-19.0	115.7	<b>-16.1</b>	<b>112.2</b>	-41.5	131.3	<b>-31.5</b>	<b>126.6</b>
H500	24	0201	-24.5	167.1	-26.1	165.6	-69.4	194.5	<b>-60.1</b>	195.1
H500	36	0201	<b>-28.5</b>	229.3	-33.8	228.5	-86.4	264.9	<b>-77.5</b>	265.7
H500	48	0201	<b>-36.7</b>	294.4	-47.1	294.1	-100.6	<b>340.5</b>	<b>-91.8</b>	344.2
H500	12	0206	-11.5	96.6	<b>-9.3</b>	<b>91.4</b>	-10.9	101.9	<b>-2.3</b>	<b>93.6</b>
H500	24	0206	-5.3	128.3	-4.5	<b>123.0</b>	-13.4	127.2	<b>-1.1</b>	<b>117.4</b>
H500	36	0206	-4.9	172.1	-6.7	<b>166.1</b>	-21.6	172.7	<b>-9.6</b>	<b>159.8</b>
H500	48	0206	<b>-2.9</b>	219.8	-9.3	<b>213.4</b>	-14.0	218.5	<b>-7.8</b>	<b>204.2</b>
H500	12	0112	-8.8	111.2	<b>-1.8</b>	<b>108.7</b>	-12.8	114.2	<b>-3.6</b>	112.9
H500	24	0112	-6.1	150.0	<b>-2.4</b>	148.3	-13.6	159.5	<b>-8.3</b>	158.2
H500	36	0112	-3.7	193.6	-4.1	<b>191.2</b>	-13.8	214.2	-12.5	214.1
H500	48	0112	<b>-0.7</b>	240.1	-6.3	<b>235.9</b>	<b>-9.9</b>	274.7	-13.5	275.7
H500	12	9912	-14.3	150.1	<b>-6.7</b>	149.3	-13.8	133.5	<b>-3.2</b>	<b>130.3</b>
H500	24	9912	-21.7	195.6	<b>-15.3</b>	194.2	-35.0	196.1	<b>-26.3</b>	<b>192.6</b>
H500	36	9912	-24.0	240.3	<b>-21.6</b>	240.0	-54.3	265.6	-52.6	264.2
H500	48	9912	<b>-26.5</b>	285.6	-28.7	287.0	<b>-71.1</b>	342.5	-77.0	340.7
T850	12	0201	-0.08	<b>0.91</b>	-0.08	0.94	-0.13	<b>0.90</b>	<b>-0.06</b>	0.95
T850	24	0201	<b>-0.12</b>	<b>1.31</b>	-0.16	1.36	-0.23	<b>1.30</b>	<b>-0.14</b>	1.35
T850	36	0201	<b>-0.16</b>	<b>1.66</b>	-0.23	1.73	-0.27	<b>1.61</b>	<b>-0.19</b>	1.69
T850	48	0201	<b>-0.18</b>	<b>2.01</b>	-0.29	2.09	-0.29	<b>1.90</b>	<b>-0.21</b>	2.00
T850	12	0206	<b>-0.04</b>	<b>0.79</b>	-0.11	0.82	-0.03	<b>0.75</b>	-0.03	0.78
T850	24	0206	<b>-0.07</b>	<b>1.08</b>	-0.19	1.13	-0.04	1.05	-0.06	1.06
T850	36	0206	<b>-0.09</b>	<b>1.34</b>	-0.26	1.40	<b>-0.06</b>	1.30	-0.09	1.29
T850	48	0206	<b>-0.10</b>	<b>1.59</b>	-0.31	1.67	<b>-0.06</b>	1.54	-0.10	<b>1.49</b>
T850	12	0112	-0.07	<b>0.85</b>	-0.07	0.91	-0.07	<b>0.86</b>	<b>-0.03</b>	0.89
T850	24	0112	<b>-0.10</b>	<b>1.20</b>	-0.13	1.28	-0.10	<b>1.21</b>	<b>-0.07</b>	1.27
T850	36	0112	<b>-0.12</b>	<b>1.48</b>	-0.20	1.57	-0.11	<b>1.50</b>	-0.09	1.60
T850	48	0112	<b>-0.13</b>	<b>1.72</b>	-0.26	1.82	<b>-0.10</b>	<b>1.77</b>	-0.12	1.91
T850	12	9912	-0.07	<b>0.95</b>	-0.08	1.00	-0.07	<b>0.89</b>	<b>0.01</b>	0.94
T850	24	9912	<b>-0.10</b>	<b>1.34</b>	-0.14	1.43	-0.11	<b>1.26</b>	<b>-0.03</b>	1.33
T850	36	9912	<b>-0.11</b>	<b>1.64</b>	-0.19	1.75	-0.15	<b>1.56</b>	<b>-0.08</b>	1.65
T850	48	9912	<b>-0.11</b>	<b>1.90</b>	-0.24	2.00	-0.18	<b>1.85</b>	<b>-0.15</b>	1.93

than DMI-HIRLAM-E. Except for the June/July 2002 period DMI-HIRLAM-E has better rms scores than DMI-HIRLAM-E-new.

Equivalent results for temperature at, e.g., 300 hPa confirm the obs-verification results in that the new versions in general do have somewhat better rms scores than the old versions in all four periods and for the forecast lengths given in the table. DMI-HIRLAM-E-new also has better bias-scores than DMI-HIRLAM-E.

### 3.3. November 2002

During November 2002, the new set-up was running in parallel in near real time. This parallel test had one difference compared to the delayed mode run tests. Due to the longer cutoff times for the start of the forecasts for the long runs at 00 UTC, 06 UTC, 12 UTC and 18 UTC, the new set-up had more observations available for the analyses in these runs. This difference is minor compared to the other differences in the general set-ups.

Obs-verification results for November 2002 for the EWGLAM stations are shown in Figure 13. In general DMI-HIRLAM-E-new has better rms-scores than DMI-HIRLAM-E while DMI-HIRLAM-G-new may score better or worse than DMI-HIRLAM-G.

A diagnostic calculation of visibility was implemented operationally with the upgrade in September 2000 (Petersen and Nielsen, 2000). Since the upgrade in April 2002 the prediction of low visibility has been rather poor. The upgrade with upstream advection of TKE and moisture fields (specific humidity and specific cloud water) has made many fields smoother than before. This is probably also the case for visibility, reducing the number of forecasted cases with local low visibility. This can be illustrated for November 2002 that had relatively many cases with very low visibility. Contingency tables of visibility for 12 and 18 h forecasts for the DMI-HIRLAM-E and DMI-HIRLAM-D versions are given in tables 14 and 15, respectively. The five classes are (visibility in km):  $V1 < 1$ ,  $1 \leq V2 < 5$ ,  $5 \leq V3 < 10$ ,  $10 \leq V4 < 20$  and  $V5 \geq 20$ .  $V$  is either F (forecast) or O (observation) as for precipitation. In the head of every “subtable” the one class error, defined as the percentage of forecasts that are within one class of the corresponding observation class, is stated as well. The following Danish SYNOP stations are included in the verification (see Figure 12 for the position of these stations): 6030, 6041, 6043, 6049, 6052, 6053, 6058, 6060, 6070, 6079, 6080, 6096, 6104, 6108, 6110, 6120, 6100, 6119, 6124, 6111, 6141, 6149, 6156, 6159, 6160, 6170, 6179, 6180, 6183, 6190, 6193. For the 12 h forecasts valid at 00 and 12 UTC the one class error as well as the total percentage of numbers in the diagonal is a little higher in DMI-HIRLAM-E/DMI-HIRLAM-E-new than in DMI-HIRLAM-D/DMI-HIRLAM-D-new. When comparing the new versions to the operational versions, the tendency is clear as the operational versions has better scores for high visibility and fewer false alarms (the F1/O5 combination) of low visibility. However, for the first 3 classes with low visibility, the new versions are much better. That also includes prediction of fog (visibility below 1 km) which is of particular concern. Both DMI-HIRLAM-E-new and DMI-HIRLAM-D-new predict 12 out of 74 cases with observed fog whereas DMI-HIRLAM-D predicts none of these. With acceptance of a 1 class error the number increases to 51 (68.9%) for DMI-HIRLAM-D-new, 38 (51.4%) for DMI-HIRLAM-E-new, 13 (17.6%) for DMI-HIRLAM-D and 29 (39.2%) for DMI-HIRLAM-E.

For 18 h forecasts valid at 06 and 18 UTC the tendency is somewhat the same. Here the

**Table 14:** Contingency tables for visibility for November 2002 of 12 h forecasts valid at 00 and 12 UTC. The numbers in parentheses are the one class error.

DMI-HIRLAM-D 200211 (73.90 %)							DMI-HIRLAM-E 200211 (75.81 %)						
	O1	O2	O3	O4	O5	sum		O1	O2	O3	O4	O5	sum
F1	0	4	1	0	0	5	F1	7	13	4	2	1	27
F2	13	29	19	15	9	85	F2	22	46	25	19	17	129
F3	28	61	54	45	33	221	F3	17	53	51	48	34	203
F4	30	253	223	234	239	979	F4	28	245	235	229	218	955
F5	3	25	54	98	258	438	F5	0	15	36	94	269	414
sum	74	372	351	392	539	1728	sum	74	372	351	392	539	1728
%FO	0	8	15	60	48	33	%FO	9	12	15	58	50	35

DMI-HIRLAM-D-new 200211 (75.35 %)							DMI-HIRLAM-E-new 200211 (78.94 %)						
	O1	O2	O3	O4	O5	sum		O1	O2	O3	O4	O5	sum
F1	12	40	25	11	14	102	F1	12	29	9	5	9	64
F2	39	74	54	54	32	253	F2	36	85	58	38	23	240
F3	15	79	89	71	66	320	F3	20	79	83	90	51	323
F4	8	171	161	191	239	770	F4	6	168	177	190	253	794
F5	0	8	22	65	188	283	F5	0	11	24	69	203	307
sum	74	372	351	392	539	1728	sum	74	372	351	392	539	1728
%FO	16	20	25	49	35	32	%FO	16	23	24	48	38	33

**Table 15:** Contingency tables for visibility for November 2002 of 18 h forecasts valid at 06 and 18 UTC. The numbers in parentheses are the one class error.

DMI-HIRLAM-D 200211 (75.19 %)							DMI-HIRLAM-E 200211 (77.07 %)						
	O1	O2	O3	O4	O5	sum		O1	O2	O3	O4	O5	sum
F1	1	1	2	0	0	4	F1	16	11	9	0	5	41
F2	35	40	37	5	11	128	F2	31	68	53	23	20	195
F3	12	63	42	36	37	190	F3	17	84	61	57	52	271
F4	33	256	222	224	218	953	F4	17	208	196	202	266	889
F5	0	15	51	109	251	426	F5	0	4	35	92	174	305
sum	81	375	354	374	517	1701	sum	81	375	354	374	517	1701
%FO	1	11	12	60	49	33	%FO	20	18	17	54	34	31

DMI-HIRLAM-D-new 200211 (74.31 %)							DMI-HIRLAM-E-new 200211 (75.49 %)						
	O1	O2	O3	O4	O5	sum		O1	O2	O3	O4	O5	sum
F1	23	45	32	7	25	132	F1	19	32	28	10	11	100
F2	42	89	74	50	47	302	F2	44	96	85	47	51	323
F3	9	81	67	66	77	300	F3	8	84	78	72	72	314
F4	7	157	158	178	215	715	F4	10	163	146	188	262	769
F5	0	3	23	73	153	252	F5	0	0	17	57	121	195
sum	81	375	354	374	517	1701	sum	81	375	354	374	517	1701
%FO	28	24	19	48	30	30	%FO	23	26	22	50	23	30

**Table 16:** Peak values observed and forecasted at given stations for Case I, Case II, Case III and Case IV.

<b>Case I:</b> high water in the Baltic Sea December 20 2001 with max. 06-08 UTC											
Station	obs	Model	0-6	6-12	12-18	18-24	24-30	30-36	36-42	42-48	48-54
Åbenrå	157	opr	91	92	87	87	84	76	82	84	76
		new	90	90	83	85	87	81	79	82	76
Gedser	121	opr	74	74	71	76	75	68	66	67	77
		new	73	73	69	72	74	67	64	66	73
<b>Case II:</b> high water in the Baltic Sea January 2 2002 with max. 14-17 UTC											
Station	obs	Model	0-6	6-12	12-18	18-24	24-30	30-36	36-42	42-48	48-54
Åbenrå	151	opr	112	111	110	109	106	108	106	103	102
		new	114	113	111	111	105	104	103	100	97
Gedser	142	opr	109	108	108	105	99	95	97	91	87
		new	108	107	105	105	103	102	102	102	98
<b>Case III:</b> storm surge in the Jutland Wadden Sea at midnight January 28/29 2002											
Station	obs	Model	0-6	6-12	12-18	18-24	24-30	30-36	36-42	42-48	48-54
Vidå	369	opr	361	371	382	370	340	325	233	219	–
		new	355	336	338	362	328	326	299	252	–
Esbjerg	336	opr	310	333	347	328	307	311	229	222	–
		new	314	309	312	312	294	297	290	253	–
Thorsminde	243	opr	187	206	223	226	228	242	169	153	–
		new	192	191	209	203	181	212	211	187	–
<b>Case IV:</b> high water in the Baltic Sea February 21 2002 at 10 in Åbenrå and 06 UTC in Gedser											
Station	obs	Model	0-6	6-12	12-18	18-24	24-30	30-36	36-42	42-48	48-54
Åbenrå	170	opr	131	132	134	130	116	118	132	137	150
		new	133	134	138	141	128	126	124	137	107
Gedser	166	opr	129	131	130	116	118	122	132	142	–
		new	128	137	140	125	120	118	136	113	–

operational versions have better one class errors compared to their new counterpart. The number of false alarms for fog is quite large for DMI-HIRLAM-D-new. The new versions have also better predictions of low visibility in this case. The same tendencies were also seen in the months before November for which the DMI-HIRLAM new set-up used a centered difference advection scheme for the moisture variables  $q$  and CW.

### 3.4. Mike21 results

The results from the storm surge model are summarized in Tables 16 and 17.



**Table 17:** Peak values observed and forecasted at given stations for Case IV and Case V.

<b>Case IV: storm surge in the Jutland Wadden Sea February 22 2002 in the evening</b>											
Station	obs	Model	0-6	6-12	12-18	18-24	24-30	30-36	36-42	42-48	48-54
Vidå	260	opr	254	251	276	281	249	286	260	276	247
		new	249	243	284	282	266	273	240	283	214
Esbjerg	239	opr	232	231	246	255	242	267	242	253	221
		new	228	229	262	268	249	256	226	270	192
Thorsminde	215	opr	165	168	184	178	170	196	163	182	153
		new	176	176	170	170	172	177	164	210	143
<b>Case IV: storm surge in the Jutland Wadden Sea February 23 2002 in the morning</b>											
Station	obs	Model	0-6	6-12	12-18	18-24	24-30	30-36	36-42	42-48	48-54
Vidå	306	opr	277	278	255	267	264	267	309	302	258
		new	268	270	259	274	254	255	263	308	250
Esbjerg	280	opr	238	239	222	236	224	234	266	273	231
		new	234	236	225	240	229	233	224	266	222
Thorsminde	243	opr	163	166	163	168	176	159	149	168	158
		new	161	160	158	168	161	159	145	158	161
<b>Case V: storm surge in the Jutland Wadden Sea December 3 1999 at 17-18 UTC</b>											
Station	obs	Model	0-6	6-12	12-18	18-24	24-30	30-36	36-42	42-48	48-54
Vidå	390	opr	386	374	389	407	420	397	271	207	–
		new	389	403	367	429	401	408	339	284	–
Ballum	435	opr	394	381	383	405	418	396	287	209	–
		new	397	409	367	443	396	408	352	291	–
Ribe	512	opr	411	385	378	377	397	425	324	210	–
		new	395	406	361	449	385	390	397	286	–
Esbjerg	394	opr	294	271	258	287	283	309	224	160	–
		new	264	279	234	330	255	263	298	228	–

For the Baltic Sea cases I and II the new and old set-up in general have the same performance.

For Case III the short forecasts (6-12 hours and 12-18 hours) give too low peak water levels by up to 30 cm compared to observed peak values with the new set-up. The operational version, however, gives acceptable values for the short forecasts. For the long forecasts the new set-up gives better forecasts. This case is further studied in section 3.5.2 as one of the case studies.

For Case IV there is no pronounced difference between the results from the two set-ups. In opposition to Case III and V, the new set-up does not give better values for the long forecasts.

For Case V the new and old set-ups in general have the same performance for the short forecasts and the new set-up in general better performance for the long forecasts.

### 3.5. Case studies

#### 3.5.1. The Danish Storm on December 3rd 1999

Figure 14 shows 30 h and 18 h forecasts and the verifying analyses valid at 18 UTC December 3 1999 for DMI-HIRLAM-E and DMI-HIRLAM-E-new. Both models are very good for this case though DMI-HIRLAM-E-new has a better phase of the center of the storm by approximately 1 h (estimated from meteograms not shown here). The Mike21 results are basically neutral for short forecasts but for long forecasts coupling to the new set-up gives better results.

#### 3.5.2. January 28th 2002 storm surge

This case produced worse high water results from Mike21 with the new set-up compared to the old set-up, and has therefore been studied in some detail with respect to 10 m wind and mslp pressure. Figure 15 shows Mike21 surges for two Wadden Sea stations, namely Esbjerg and Vidå with observed peak water levels of 336 cm and 369 cm, respectively. (See also Table 16). The difference in peak value for 24 h forecasts is somewhat smaller than the difference in peak value for 18 h forecasts. Since the observed peak values are around midnight, the 18 h forecast is based on DMI-HIRLAM forecasts starting from analyses valid 06 UTC and we will focus on these forecasts. Figures 16-18 shows 6 h, 12 h, and 18 h forecasts and verifying analyses of mslp and 10 m wind valid at 12 UTC, 18 UTC or 24 UTC January 28 2002. The forecasts starts from analyses valid at 06 UTC January 28. These plots indicate that the new version has at least the same quality in the North Sea as the operational version for the forecasts shown. A subjective validation of the +18h forecasts gives the highest score to DMI-HIRLAM-E-new (Figure 18). Meteograms (not shown) for some Jutland coastal SYNOP stations of forecasts starting from 06 UTC January 28 show that the two versions have very similar 10 m wind speeds with one version having slightly more wind than the other for some forecast lengths and vice versa for other forecast lengths. However, they also show that the wind speeds at these stations start to decrease approximately one hour earlier in the DMI-HIRLAM-E-new forecasts than in the DMI-HIRLAM-E forecasts and the start time for the decrease in the observed wind speed is in between. Thus, the old set-up has one hour more of piling up water. Closer examination of the forecasted and observed water level starting from 06 UTC January 28 for the Esbjerg and Vidå stations, shown in Figure 19, show that Mike21 has the peak

value later for the old version than for the new version. The phase, however, is better for the new version. Up to the time of the observed maxima the two versions perform similar but the old version continues to increase the water level due to the later fall off of the wind which most likely is wrong. So, in reality both models seem to have too small wind speeds in the forecasts starting from 06 UTC and the old version have larger peak values, but not because of better DMI-HIRLAM forecasts. The new version gives an almost constant water level in Esbjerg between 02 UTC and 04.30 UTC as observed whereas the old version has a falling water level during this period. A similar examination of the 18 h Mike21 forecasts starting from 00 UTC shows to a large extent the same tendency with a somewhat better phase of the water level from the run with the new set-up compared to the run with the old set-up.

### 3.5.3. June 18th 2002 large precipitation

On this day thunderstorms developed ahead of a northeastward moving upper-level trough over the United Kingdom. A number of these storms passed Denmark in the afternoon and evening, giving large amounts of precipitation locally. Observations, including satellite information, indicate that two multicell storms moved across the northwestern part of Jutland, the first early in the afternoon and the second late in the afternoon (see Nielsen and Rasmussen, 2002; Amstrup *et al.*, 2003 for more detailed descriptions of the weather situation). This makes the case particularly interesting as a test case for the parameterization of moist processes in DMI-HIRLAM for at least two reasons. First, multicell storms are organized deep convective systems, strongly influenced by the vertical shear of the environmental (background) wind. Second, multicell storms have horizontal scales that are comparable to the horizontal resolution of DMI-HIRLAM-E. Therefore, this case may give a hint about how well the dynamics and the parameterization of moist processes in the model handles the regime of partly resolved deep convection having significant interaction with the environmental wind.

Figure 20 shows the 12 h (6-18 hour) forecasted accumulated precipitation for DMI-HIRLAM-E and DMI-HIRLAM-E-new, and the observed 12 h accumulated precipitation from SYNOP stations as well as from selected SVK (Spildevandskomiteen) stations; all valid at 18 UTC June 18. The predicted amounts are far too low in the old version DMI-HIRLAM-E whereas the new version DMI-HIRLAM-E-new has large precipitation amounts in parts of Jutland and along the Skagerrak coast of Norway. Considering the difficulty in forecasting such convective weather situations, the DMI-HIRLAM-E-new forecast is very good.

### 3.5.4. July 10-11 2002 large precipitation

In this period an upper-level trough moved northeastward across the North Sea. Thunderstorms that developed mainly below the right entrance region of an upper-level jet streak downstream of the upper-level trough (Figure 21) gave locally large amounts of precipitation. On July 10 large amounts of precipitation, accumulated from 18 to 06 UTC, were measured in a band from south-southeast to north-northwest over northern Germany, Denmark and southern Norway (Figure 22, bottom row). At some locations in Denmark the accumulated precipitation exceeded 50 mm. Both the operational DMI-HIRLAM-E and DMI-HIRLAM-D and the corresponding versions DMI-HIRLAM-E-new and DMI-HIRLAM-D-new predicted the precipitation band fairly well (Figure 22, middle and upper row). However, the predicted

amounts were too low in the operational set-up, particularly in DMI-HIRLAM-E, while the predicted amounts in the new set-up were in the observed range. The phase of the band with predicted maximum accumulated precipitation also appeared to be in somewhat better agreement with the observations in the new set-up than in the operational set-up (Figure 22).

### 3.5.5. November 25-26 2002 large precipitation

This test case is from the period with pre-operational testing of the new set-up and illustrates the ability of DMI-HIRLAM-E-new to produce large amounts of precipitation in late autumn/early winter in Northern Italy and Switzerland. Figure 23 shows 12h forecasted precipitation and Figure 24 shows the observed values from SYNOP stations on the GTS valid on 06 UTC November 26 2002. The largest observed value is 83 mm in the southern part of Switzerland and other large amounts are observed nearby with some variability. In Genova 45 mm is observed but there is no nearby observations so it is not known whether this is the extreme value or if larger amounts of precipitation has fallen in the areas with no (SYNOP on GTS) observations. Also some precipitation is observed in the region near the Italian/Austrian/Slovenian borders.

The operational forecasts are rather bad but with some indication of large amounts of precipitation in the 30 h-42 h forecast range. The DMI-HIRLAM-E-new forecasts are better in the sense that it predicts somewhat higher values and also the position of the larger amounts are better and becoming better, with decreasing forecast length. Note the decrease in the amounts with decreasing forecast lead times from too large to slightly too small amounts.

## 4. Conclusion

The performance of the new model system in five storm surge cases has been compared with the performance of the old system for the same cases. It was found that the quality of the predicted water levels at the coasts of the Danish Waters generally was at the same level in the two systems. However, a tendency for somewhat better prediction of the water level in long forecasts (i.e. beyond 18 h) with the new system was noted.

A clear improvement in the prediction of the vertical profile of temperature was noted in the new set-up. The old forecasting system had a systematic tendency to increase the bulk static stability of the troposphere with increasing forecast lead time. The stabilization was mainly due to warming at upper levels in the troposphere. The upper-level warming was most pronounced in the summer period. In the new system the tendency for upper-tropospheric warming in the summer period was practically eliminated. The change in the vertical temperature profile was related to a significant change in the predicted precipitation. The change occurred mainly in the predicted convective precipitation. The number of predicted cases with small 12 hour accumulated precipitation amounts ( $< 0.2$  mm) and the corresponding number of heavy precipitation cases ( $\geq 10$  mm) were both increased. The increase in the predicted small amounts of precipitation is a drawback, since the DMI-HIRLAM system overpredicts this precipitation class. However, the overprediction of class O1/F1 by the new set-up is less than it was prior to the previous upgrade involving upstream advection of the moisture variables and TKE, here referred to as the operational or old set-up. Case studies, two Danish

summer cases and one Mediterranean autumn case, showed a remarkable improvement in the prediction of heavy (convective) precipitation by the new set-up.

It was also shown that the relative humidity (rh) near the surface in the new set-up was increased to a level in much better agreement with the observations. This change was particularly clear for the summer periods in a verification against Danish land stations.

The improved prediction of near-surface rh also leads to a clear improvement of the predicted near-surface visibility in the range from 0 to 5 km. However, as a drawback the false alarm rate for the prediction of fog (visibility < 1 km) went up relative to the corresponding false alarm rate in the old set-up.

In order to maintain a very high computational stability it was found necessary to decrease the time step by about 40 %.

## References

- Amstrup, Bjarne. 2003. *Impact of NOAA16 and NOAA17 ATOVS AMSU-A radiance data in the DMI-HIRLAM 3D-VAR analysis and forecasting system — January and February 2003*. DMI Scientific Report 03-06. Danish Meteorological Institute.
- Amstrup, Bjarne, Jørgensen, Jess U. and Sass, Bent Hansen. 2002. *DMI-HIRLAM parallel tests during first quarter of 2002*. DMI Internal Report 02-06. Danish Meteorological Institute.
- Amstrup, Bjarne, Nielsen, Niels Woetmann and Sass, Bent Hansen. 2003. *DMI-HIRLAM parallel tests with upstream and centered difference advection of the moisture variables for a summer and winter period in 2002*. DMI Scientific Report 03-03. Danish Meteorological Institute.
- Gustafsson, N., Berre, L., Hörnquist, S., Huang, X.-Y., Lindskog, M., Navascués, B., Mogensén, K. S. and Thorsteinsson, S. 2001. Three-dimensional variational data assimilation for a limited area model. Part I: General formulation and the background error constraint. *Tellus*, **53A**, 425–446.
- Kuo, H. L. 1974. Further Studies of the Parameterization of the Influence of Cumulus Convection on Large-Scale Flow. *J. Atmos. Sci.*, **31**, 1232–1240.
- Lindskog, M., Gustafsson, N., Navascués, B., Mogensén, K. S., Huang, X.-Y., Yang, X., Andræ, U., Berre, L., Thorsteinsson, S. and Rantakokko, J. 2001. Three-dimensional variational data assimilation for a limited area model. Part II: Observation handling and assimilation experiments. *Tellus*, **53A**, 447–468.
- Nielsen, Jacob Woge. 2001. *DMIs operationelle stormflodsvarslingssystem Version 2.0*. DMI Technical Report 01-02. Danish Meteorological Institute.
- Nielsen, Niels Woetmann and Rasmussen, Leif. 2002. Uvejret den 18. juni 2002. *Vejret*, **92+93**, 1–23.

- Petersen, Claus and Nielsen, Niels W. 2000. *Diagnosis of visibility in DMI-HIRLAM*. Scientific Report 00-11. Danish Meteorological Institute.
- Sass, B. H. 2002. *A research version of the STRACO cloud scheme*. DMI Technical Report 02-10. Danish Meteorological Institute.
- Sass, B. H. and Yang, Xiaohua. 2002. Recent tests of proposed revisions to the STRACO cloud scheme. *Hirlam Newsletter*, **41**, 167–174.
- Sass, Bent H., Rontu, Laura and Räisänen, Petri. 1994. HIRLAM-2 Radiation Scheme: Documentation and Tests. *HIRLAM Tech. Report*, **16**, 1–43.
- Sass, Bent Hansen. 2001. Modelling of the time evolution of low tropospheric clouds capped by a stable layer. *HIRLAM Technical Report*, **50**.
- Sass, Bent Hansen, Nielsen, Niels Woetmann, Jørgensen, Jess U., Amstrup, Bjarne, Kmit, Maryanne and Mogensen, Kristian S. 2002. *The Operational DMI-HIRLAM System - 2002 version*. DMI Technical Report 02-5. Danish Meteorological Institute.
- Savijärvi, Hannu. 1990. Fast Radiation Parameterization Schemes for Mesoscale and Short-Range Forecast Models. *J. Appl. Meteor.*, **29**, 437–447.
- Schyberg, Harald, Landelius, Tomas, Thorsteinsson, Sigurdur, Tvetter, Frank Thomas, Vignes, Ole, Amstrup, Bjarne, Gustafsson, Nils, Järvinen, Heikki and Lindskog, Magnus. 2003. Assimilation of ATOVS data in the HIRLAM 3D-VAR System. *HIRLAM Technical Report*, **60**.
- Sundqvist, H. 1993. Inclusion of ice phase of hydrometers in cloud parameterization for mesoscale and large-scale models. *Beitr. Phys. Atmosph.*, **66**, 137–147.
- Undén, P. and Gustafsson, N. 2001. Manipulations to determine the hybrid coordinate in HIRLAM. *Hirlam Newsletter*, **41**, 119–124.
- Undén, Per, Rontu, Laura, Järvinen, Heikki, Lynch, Peter, Calvo, Javier, Cats, Gerard, Cuxart, Joan, Eerola, Kalle, Fortelius, Carl, Garcia-Moya, Jose Antonio, Jones, Colin, Lenderlink, Geert, McDonald, Aidan, McGrath, Ray, Navascues, Beatrix, Nielsen, Niels Woetmann, Ødegaard, Viel, Rodriguez, Ernesto, Rummukainen, Markku, Rõõm, Rein, Sattler, Kai, Sass, Bent Hansen, Savijärvi, Hannu, Schreuer, Ben Wichers, Sigg, Robert, The, Han and Tijn, Aleksander. 2003. *HIRLAM-5 Scientific Documentation*. HIRLAM Scientific Report.

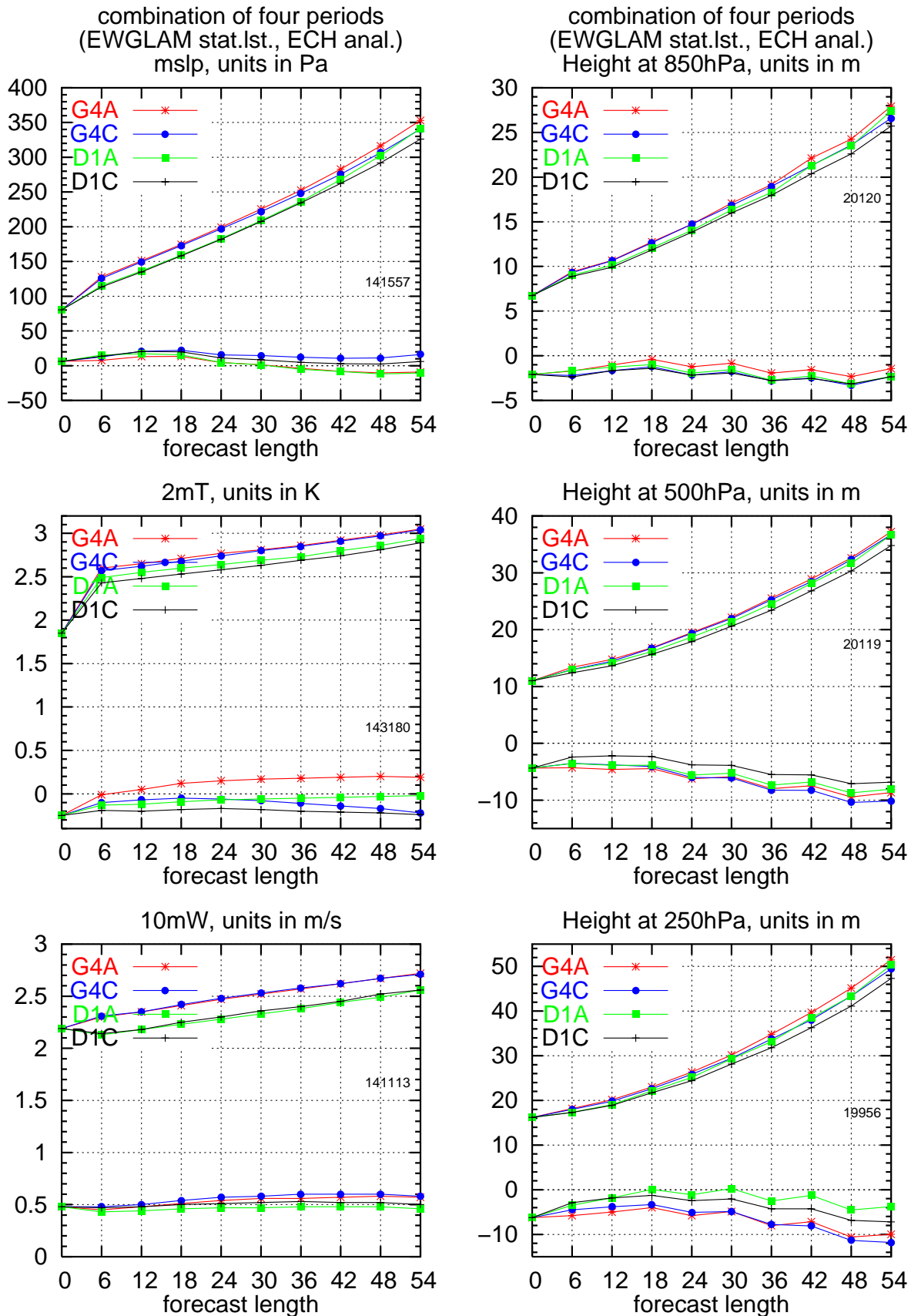


**Figure 4:** Verification (EWGLAM station list) of DMI-HIRLAM-G (G4A), DMI-HIRLAM-G-new (G4C), DMI-HIRLAM-E (D1A) and DMI-HIRLAM-E-new (D1C) of surface parameters and height for specified pressure levels. Forecasts starting from all the major SYNOP hours 00, 06, 12 and 18 UTC are included. ECMWF analyses are used. The small numbers in the plots indicate the number of observations used in the statistics.

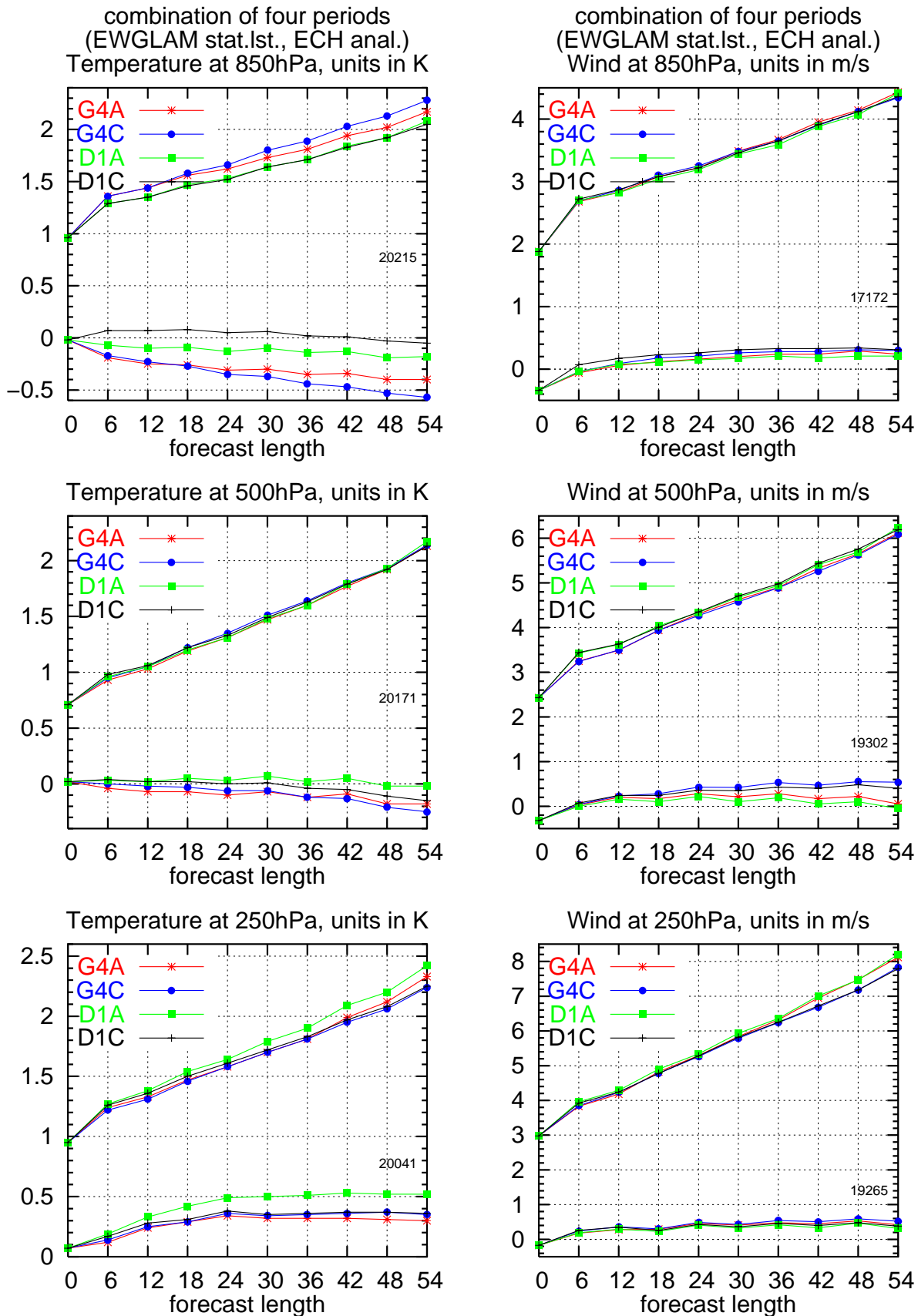


**Figure 5:** Verification (EWGLAM station list) of DMI-HIRLAM-G (G4A), DMI-HIRLAM-G-new (G4C), DMI-HIRLAM-E (D1A) and DMI-HIRLAM-E-new (D1C) of temperature and wind for specified pressure levels. Forecasts starting from all the major SYNOP hours 00, 06, 12 and 18 UTC are included. ECMWF analyses are used. The small numbers in the plots indicate the number of observations used in the statistics.



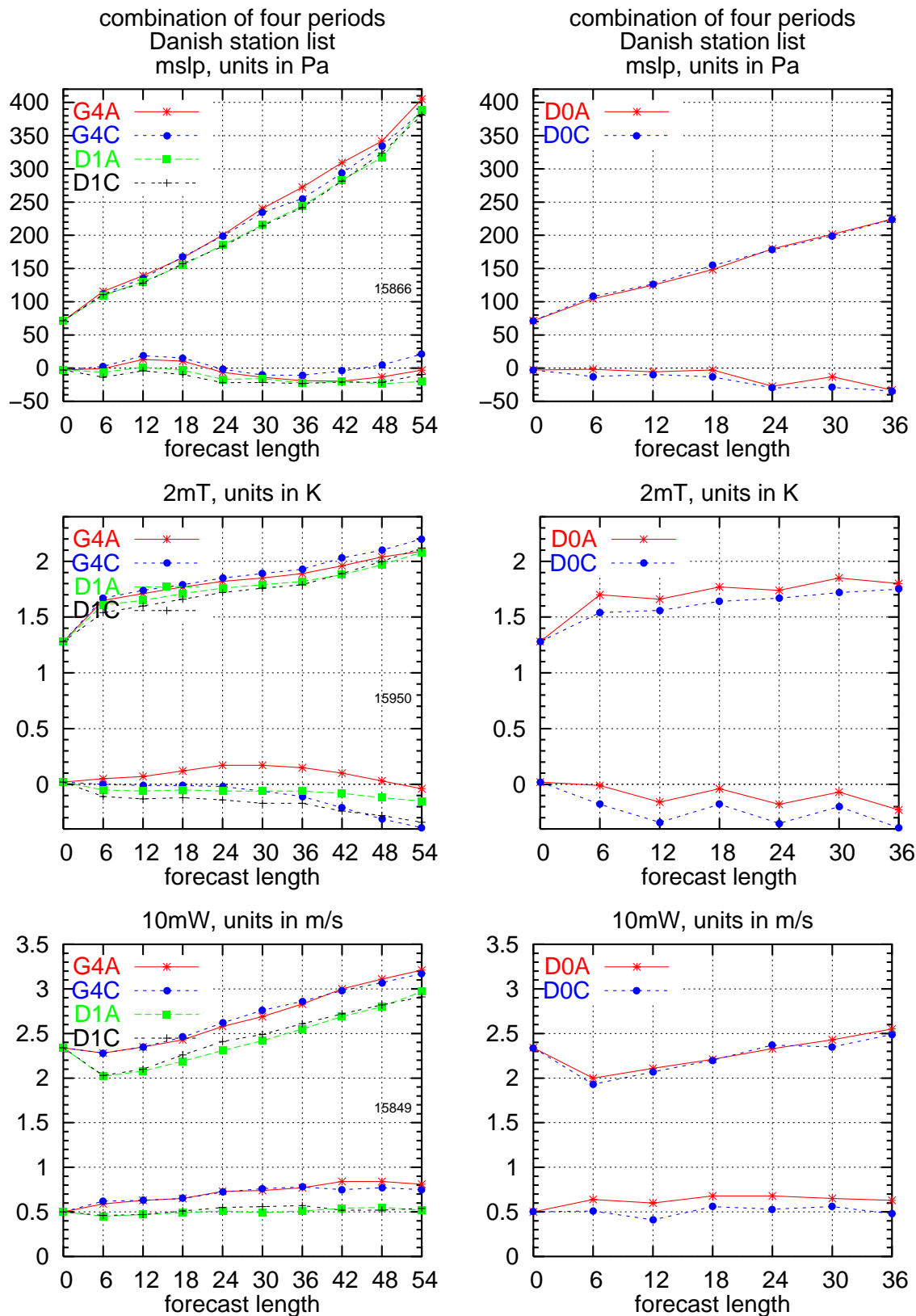


**Figure 6:** Verification (Danish station list) of DMI-HIRLAM-G (G4A), DMI-HIRLAM-G-new (G4C), DMI-HIRLAM-E (D1A) and DMI-HIRLAM-E-new (D1C) (left side) of surface parameters specified in the plot. Forecasts starting from all the major SYNOP hours 00, 06, 12 and 18 UTC are included. ECMWF analyses are used. To the right verification (Danish station list) of DMI-HIRLAM-D (D0A) and DMI-HIRLAM-D-new (D0C). Forecasts starting from the major SYNOP hours 00 and 12 UTC are included. The small numbers in the plots indicate the number of observations used in the statistics.

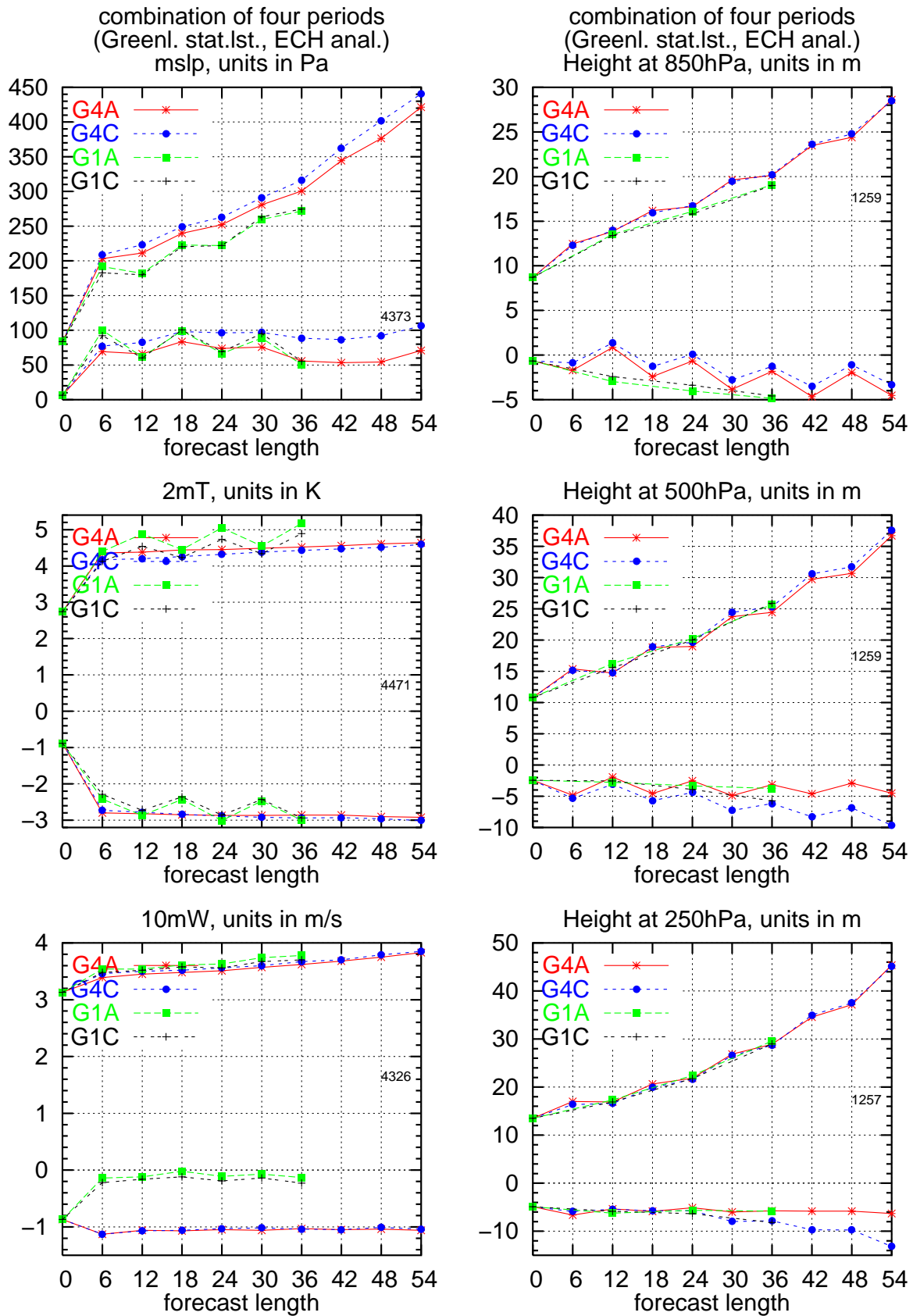


**Figure 7:** Verification (Greenland station list) of DMI-HIRLAM-G (G4A), DMI-HIRLAM-G-new (G4C), DMI-HIRLAM-N (G1A) and DMI-HIRLAM-N-new (G1C) of surface parameters and height for specified pressure levels. Forecasts starting from all the major SYNOP hours 00, 06, 12 and 18 UTC are included for G4A and G4C and forecasts starting from the major SYNOP hours 00 and 12 UTC are included for G1A and G1C. ECMWF analyses are used. The small numbers in the plots indicate the number of observations used in the statistics for G4A and G4C.

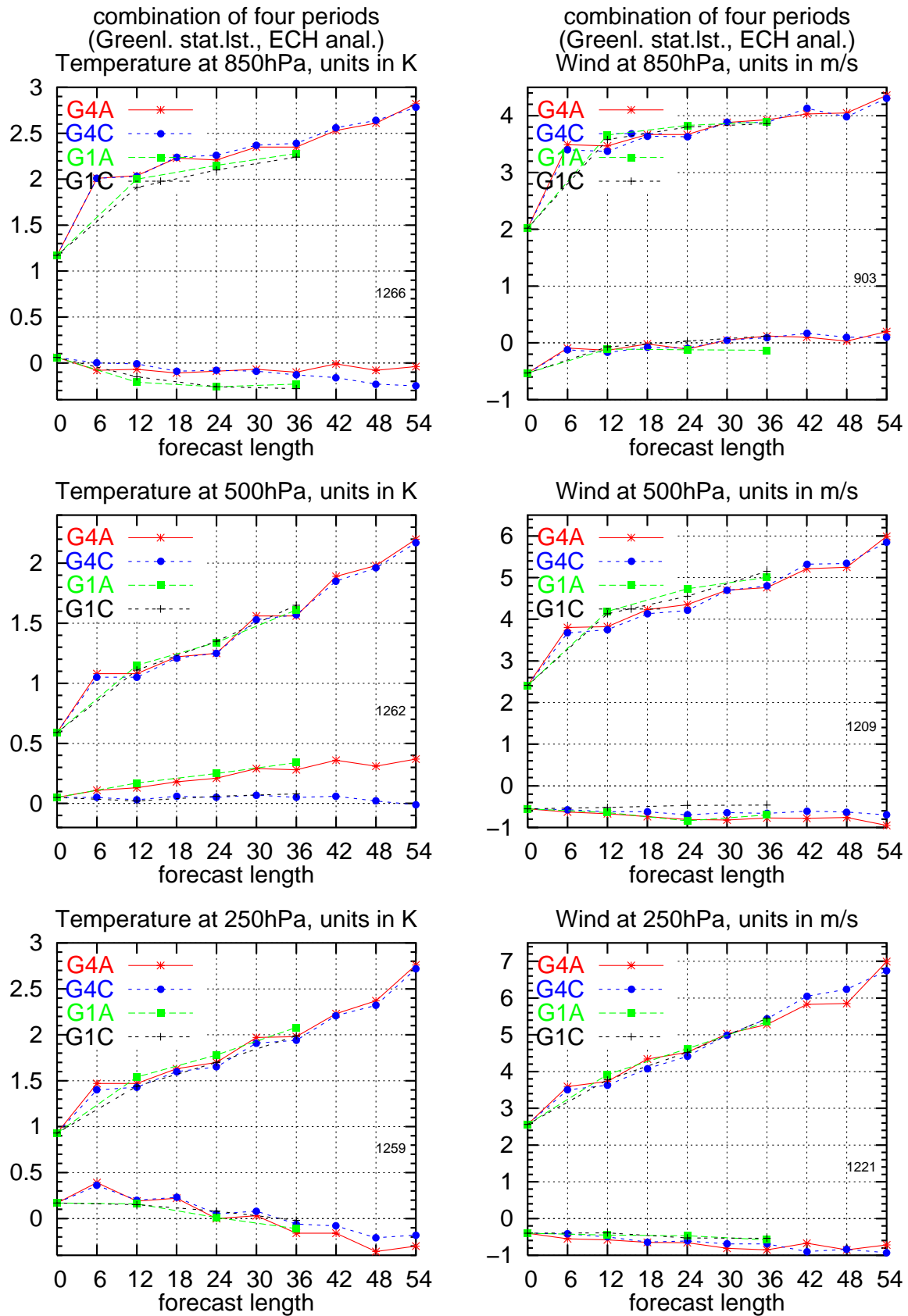


**Figure 8:** Verification (Greenland station list) of DMI-HIRLAM-G (G4A), DMI-HIRLAM-G-new (G4C), DMI-HIRLAM-N (G1A) and DMI-HIRLAM-N-new (G1C) of temperature and wind for specified pressure levels. Forecasts starting from all the major SYNOP hours 00, 06, 12 and 18 UTC are included for G4A and G4C and forecasts starting from the major SYNOP hours 00 and 12 UTC are included for G1A and G1C. ECMWF analyses are used. The small numbers in the plots indicate the number of observations used in the statistics for G4A and G4C.

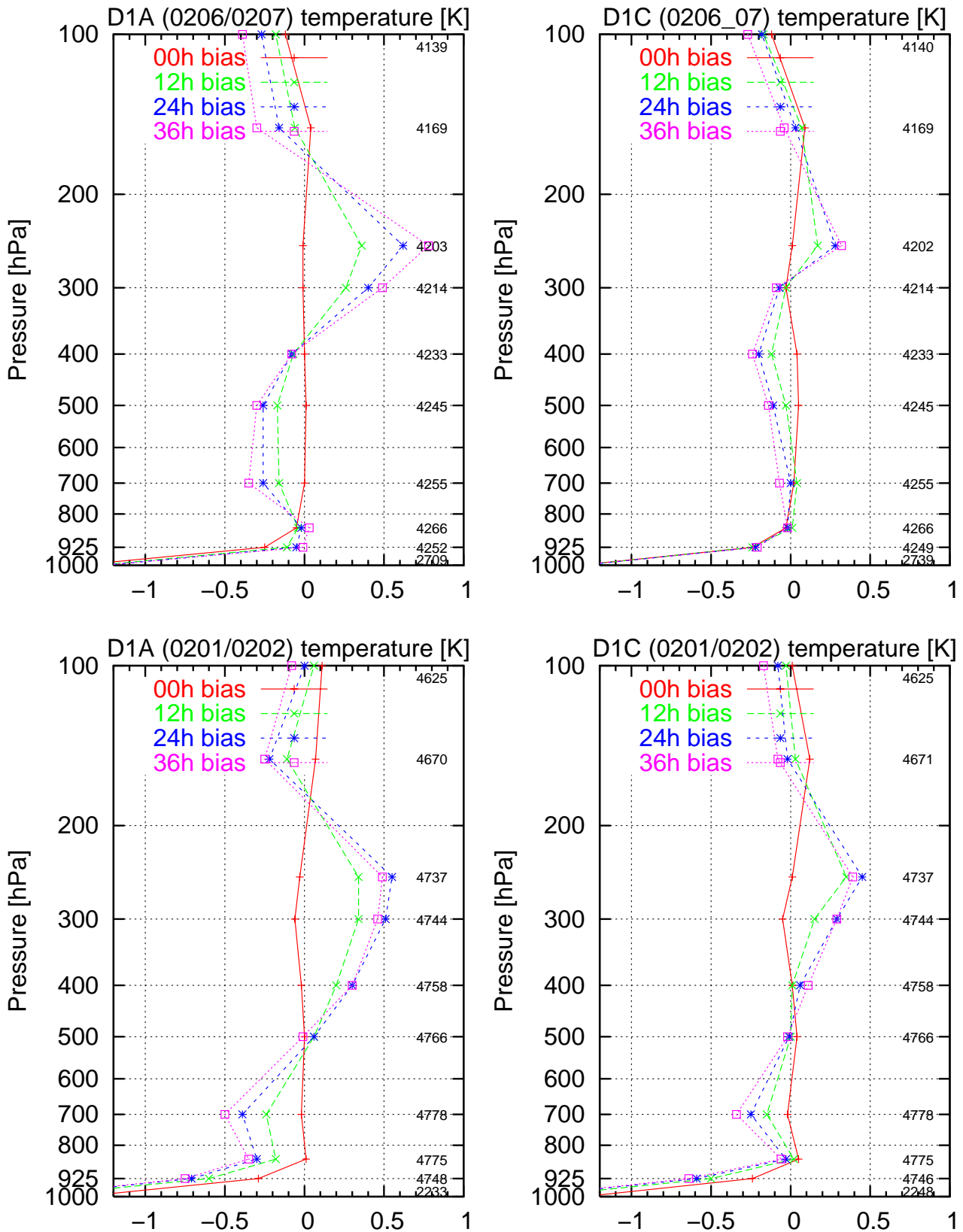


**Figure 9:** Bias scores of temperature at analysis time and for the 12, 24 and 36 hour forecasts of DMI-HIRLAM-E (D1A, left) and DMI-HIRLAM-E-new (D1C, right) as a function of pressure in the January/February 2002 period (bottom) and in the June/July 2002 period (top). (The numbers in small print in the plots indicate the number of observations used).

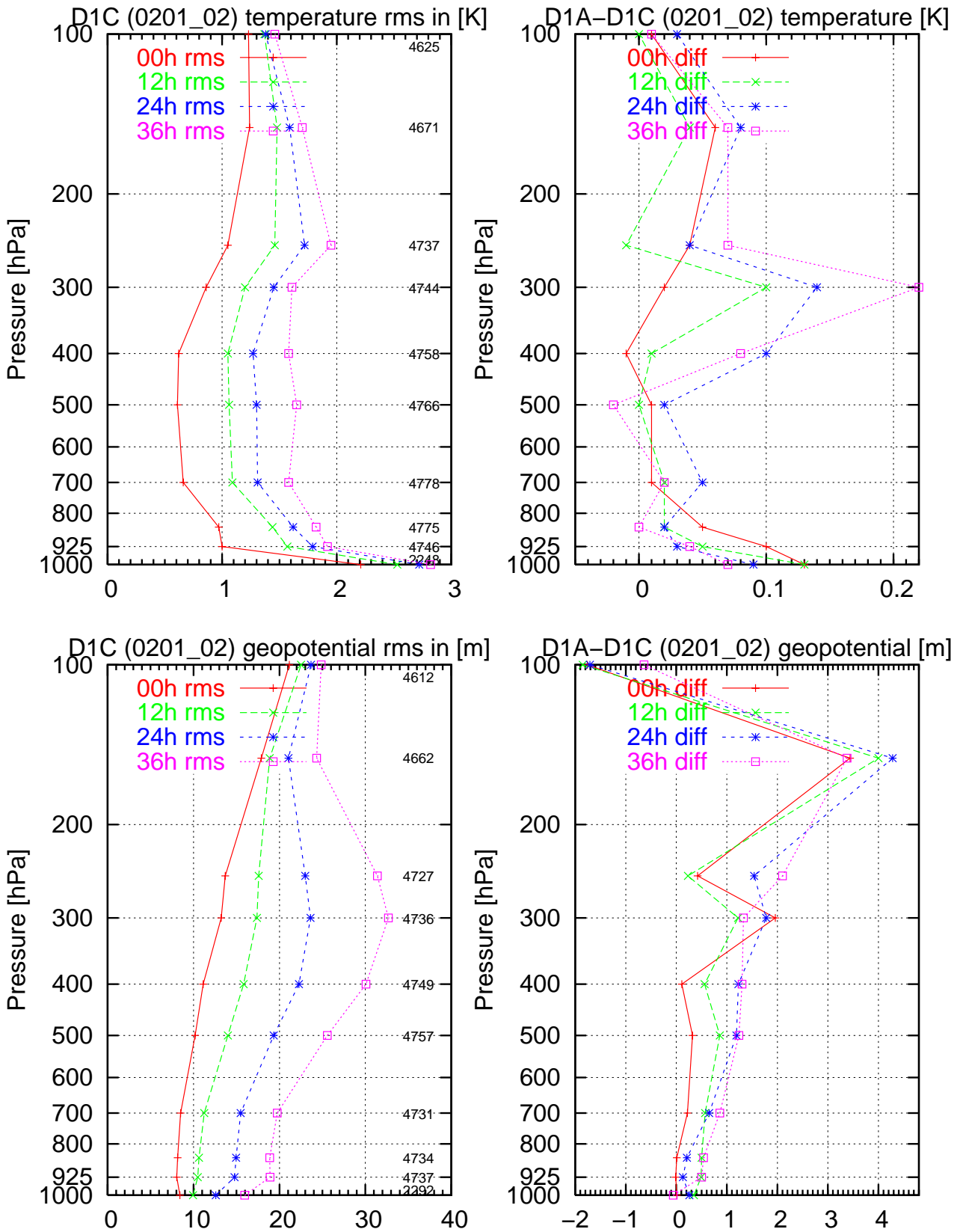


**Figure 10:** Rms scores for DMI-HIRLAM-E-new (D1C, left) and differences in rms-scores between DMI-HIRLAM-E (D1A) and DMI-HIRLAM-E-new (D1C) (right) at analysis time and for the 12, 24 and 36 hour forecasts as a function of pressure in the January/February 2002 period. Top row is for temperature and bottom row is geopotential. Positive values in the difference plots where D1C has better rms-scores.

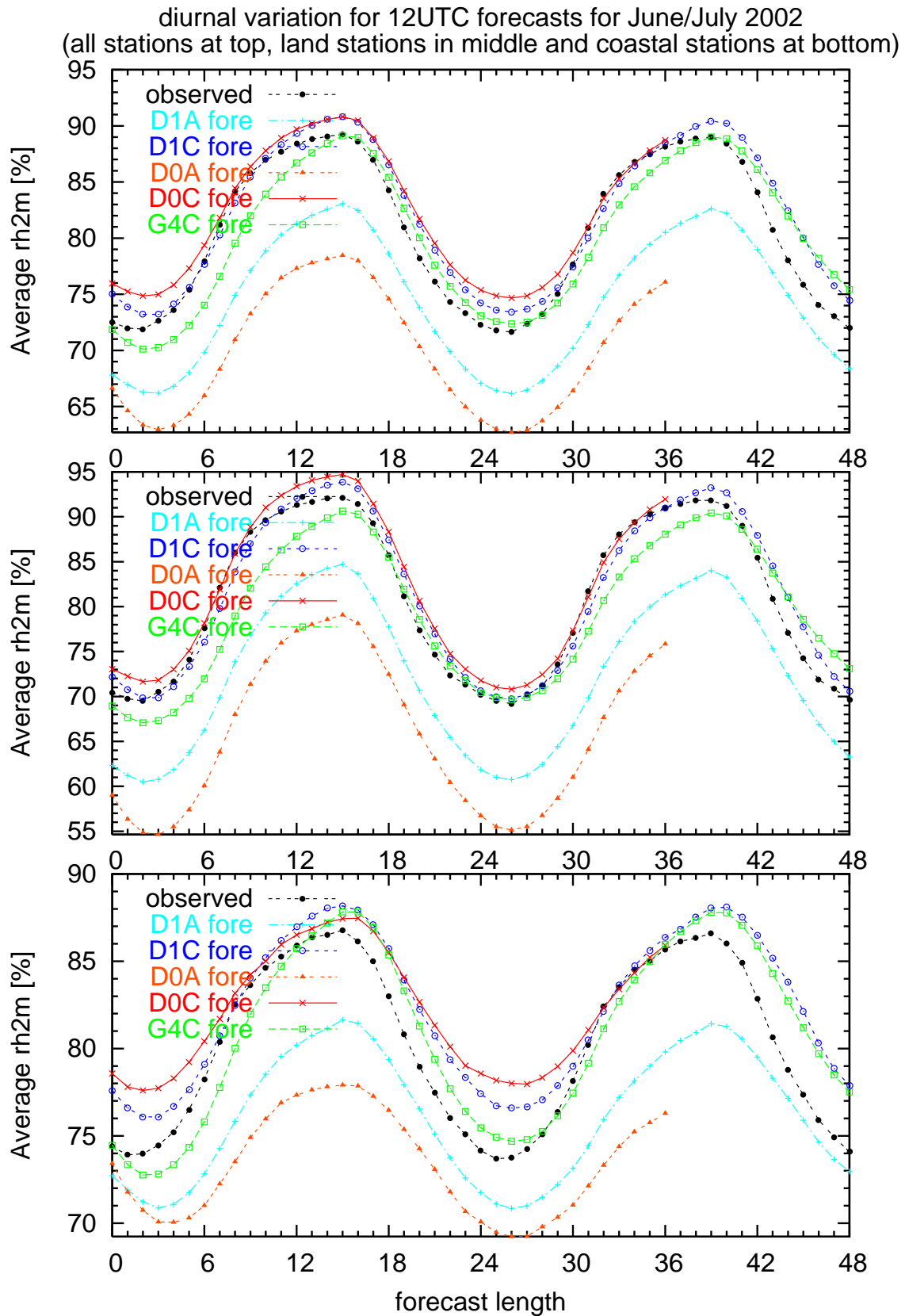


**Figure 11:** Diurnal variation for forecasts starting from 12 UTC for 2 m relative humidity for a number of Danish SYNOP stations reporting (at least) hourly. The statistics for coastal stations at bottom, land stations in middle and the combined coastal and land stations at top.

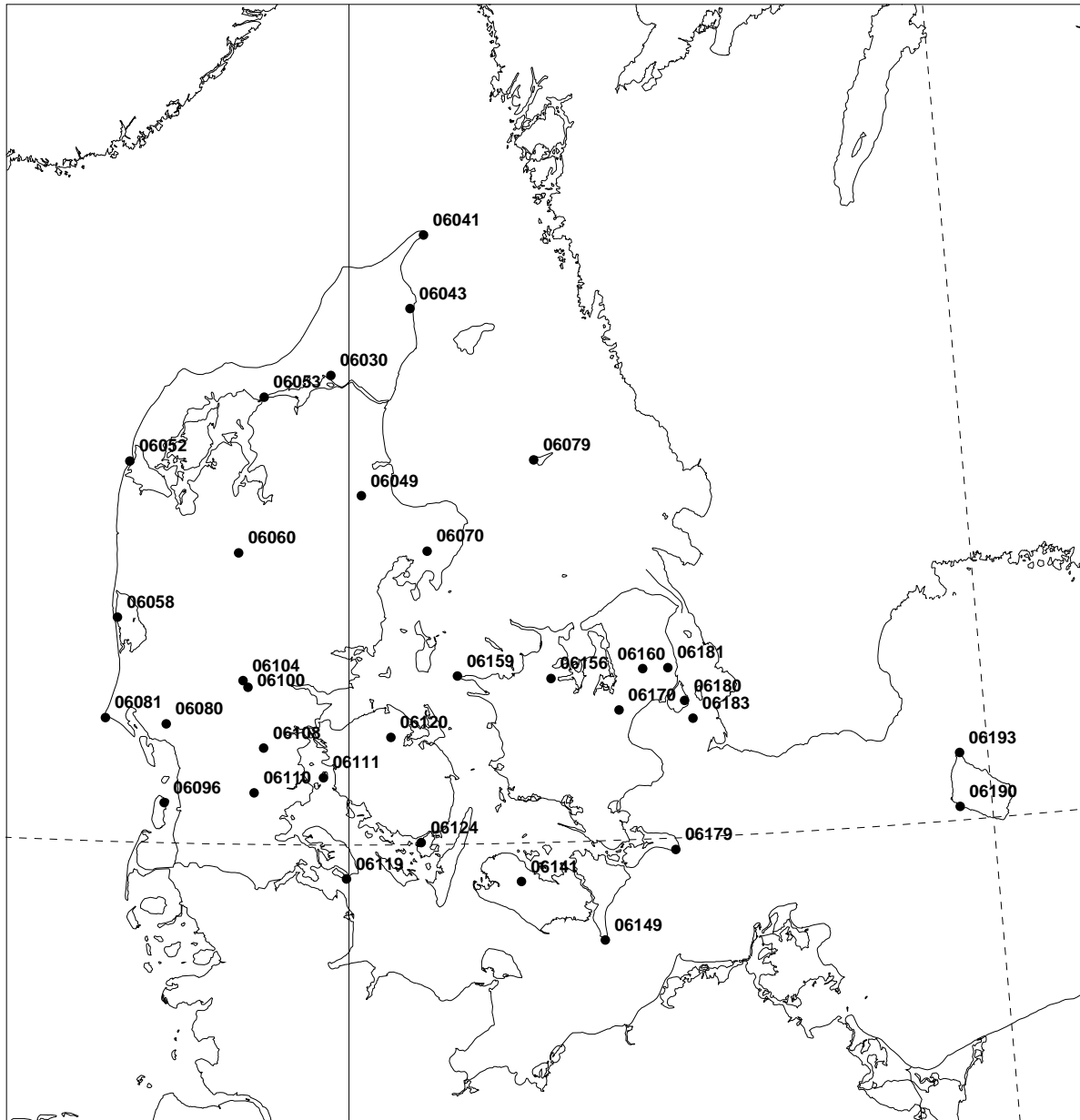


**Figure 12:** Position of stations used for either precipitation and/or visibility verification.

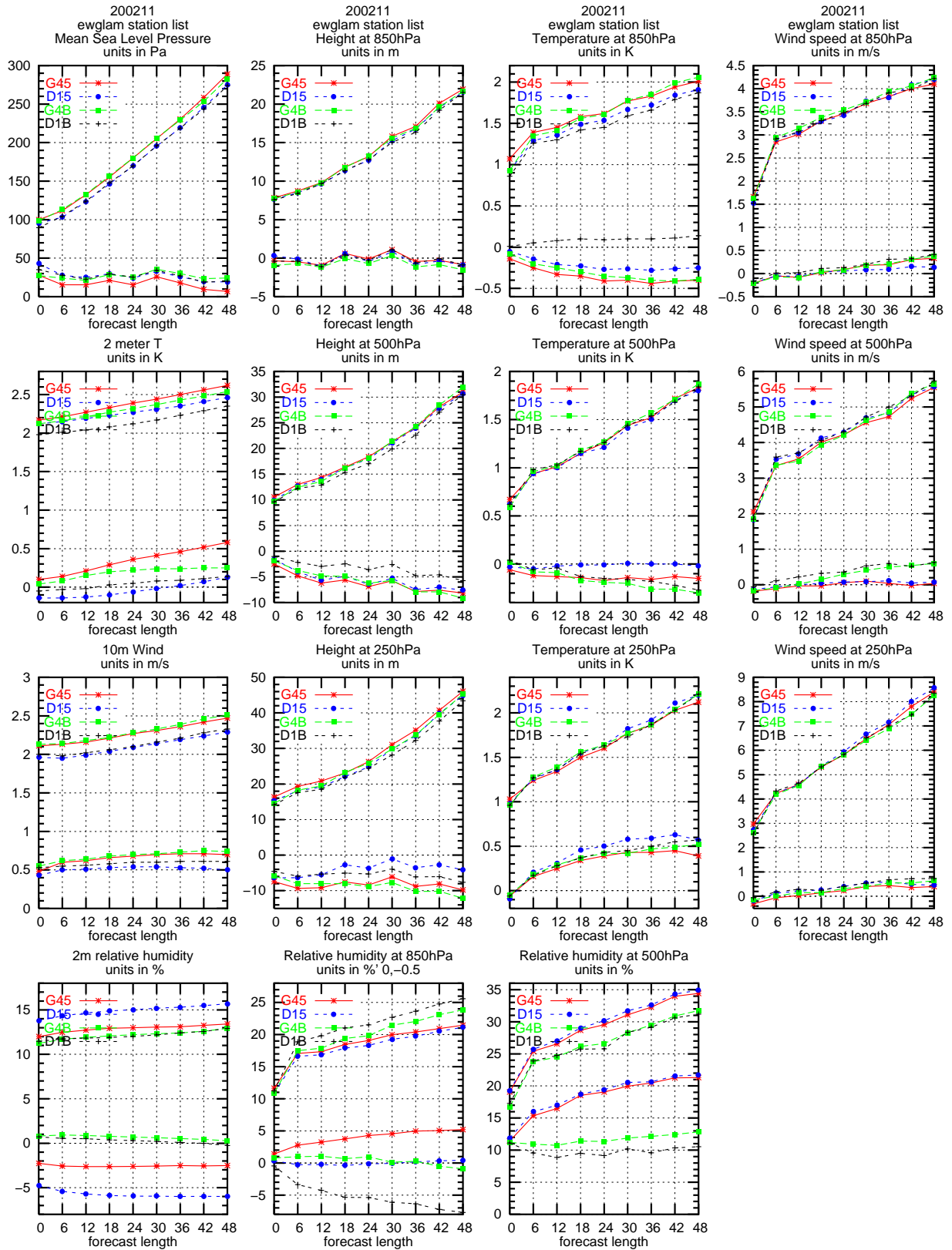


**Figure 13:** Verification (EWGLAM station list) of DMI-HIRLAM-G (G45), DMI-HIRLAM-G-new (G4B), DMI-HIRLAM-E (D15) and DMI-HIRLAM-E-new (G4B) of surface parameters and temperature, wind, humidity and height for specified pressure levels. Forecasts starting from all the major SYNOP hours 00, 06, 12 and 18 UTC are included.



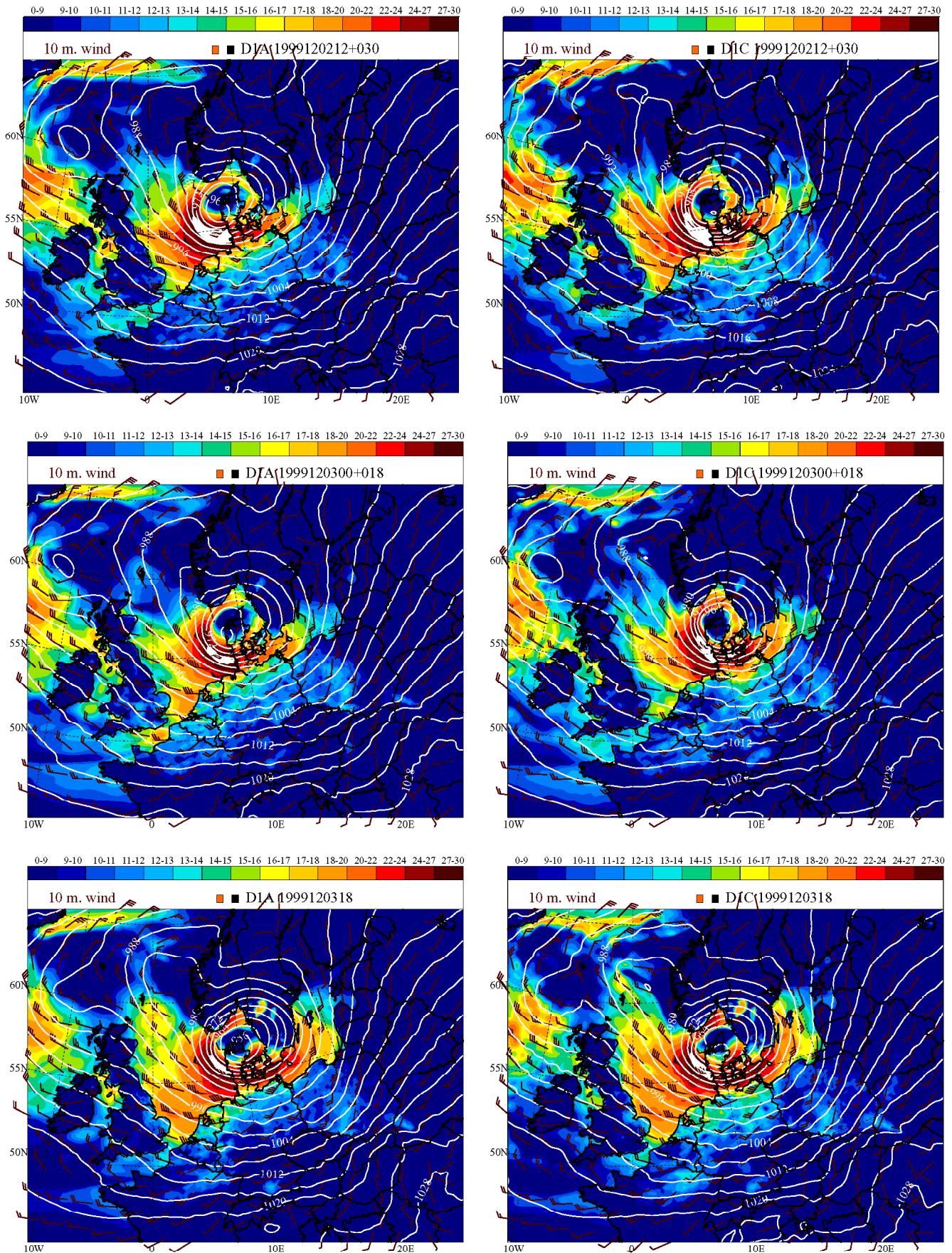


**Figure 14:** Operational DMI-HIRLAM-E (left) and new DMI-HIRLAM-E (right) mslp and 10 m wind speed valid on 18 UTC December 3, 1999. Upper row is 30 hour forecasts, middle row is 18 hour forecasts and lower row the verifying analyses.

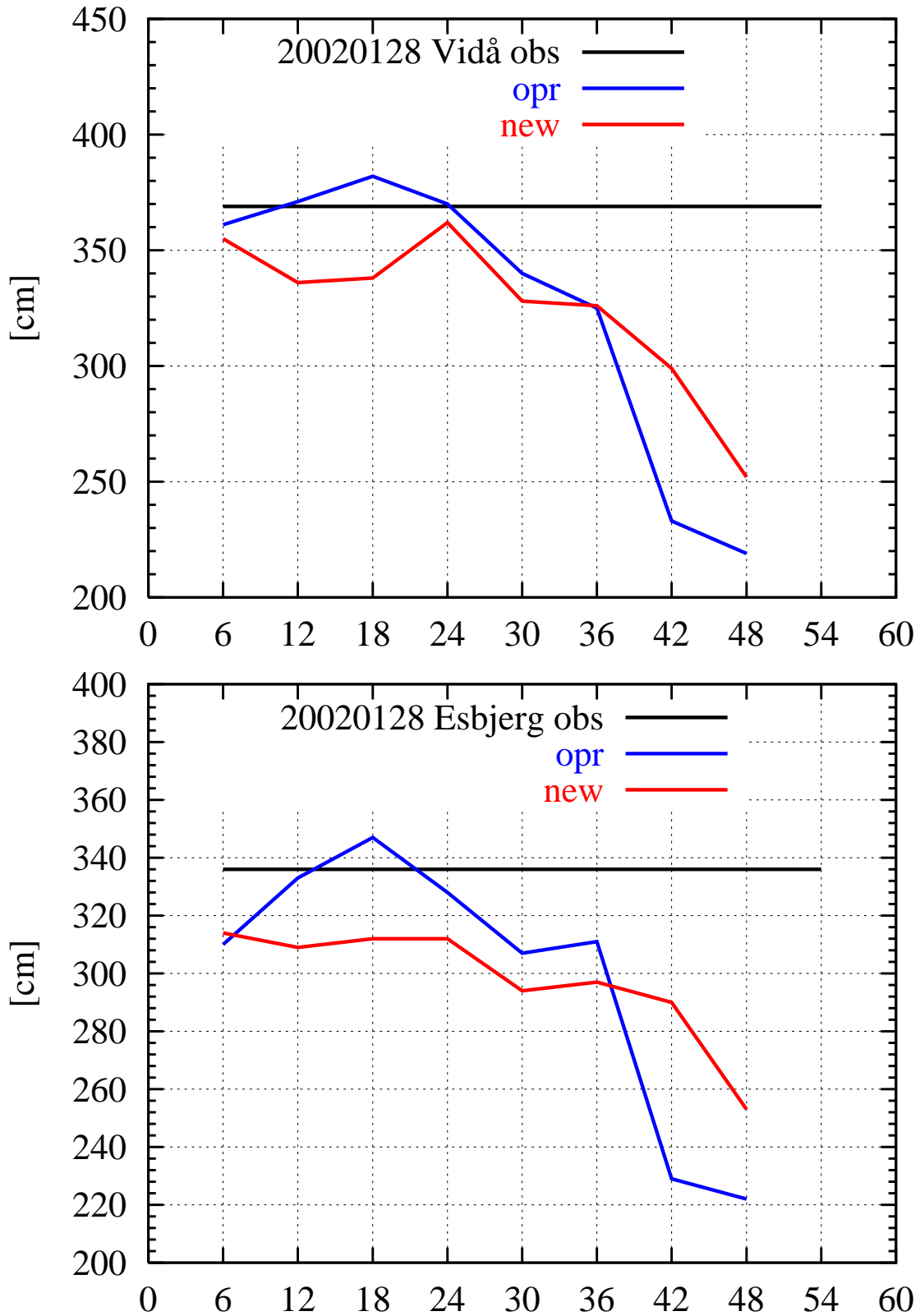


**Figure 15:** Results of peak values from Mike21 runs with the operational set-up (opr, blue curve) and the new set-up (new, red curve) for Vidå (upper) and Esbjerg (lower) for the maximum observed water level (black curve) around midnight January 28/29 2002.

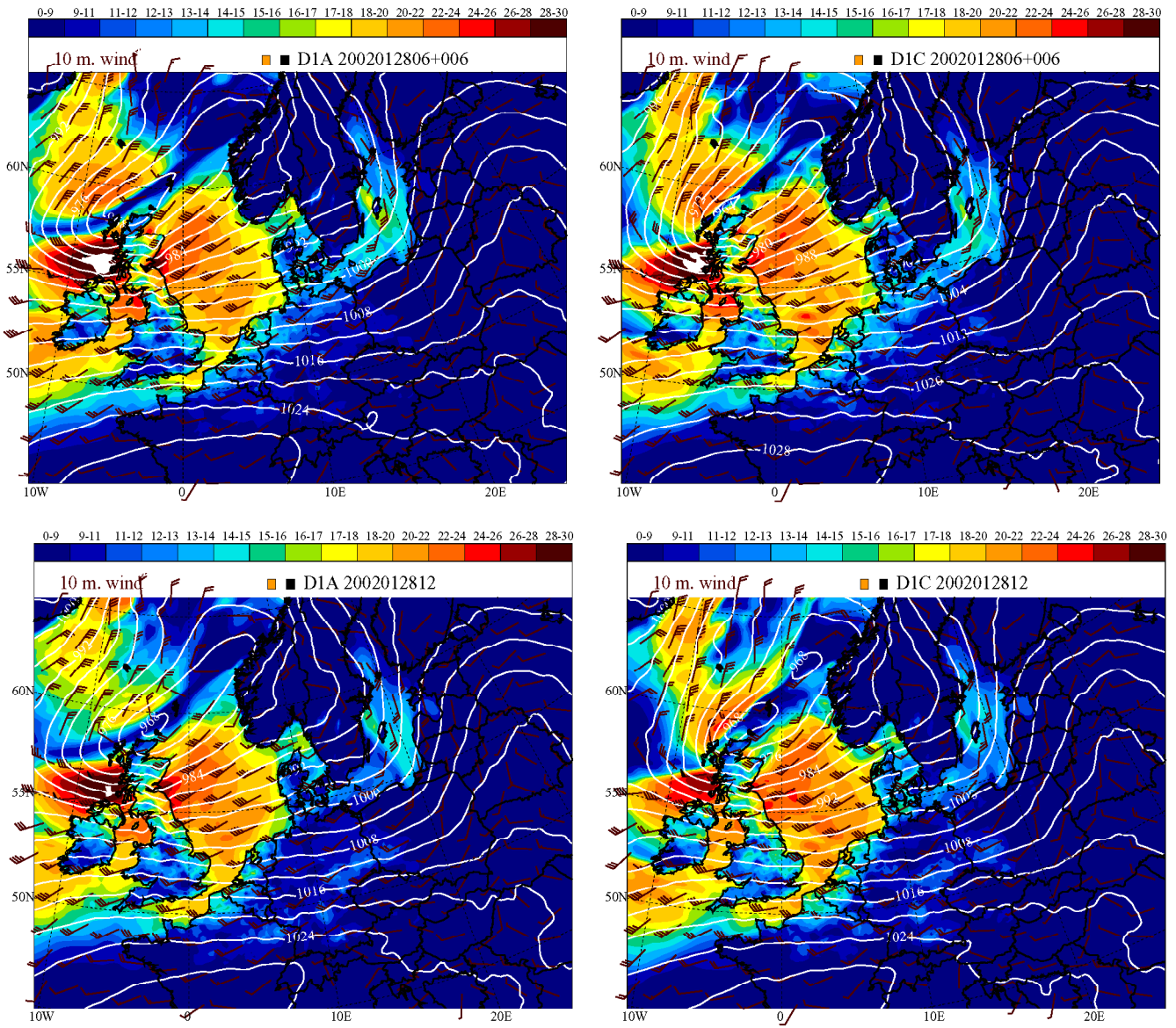


**Figure 16:** Operational DMI-HIRLAM-E (left) and new DMI-HIRLAM-E (right) mslp and 10 m wind speed valid on 12 UTC January 28, 2002. Upper row is 6 hour forecasts and lower row the verifying analyses.

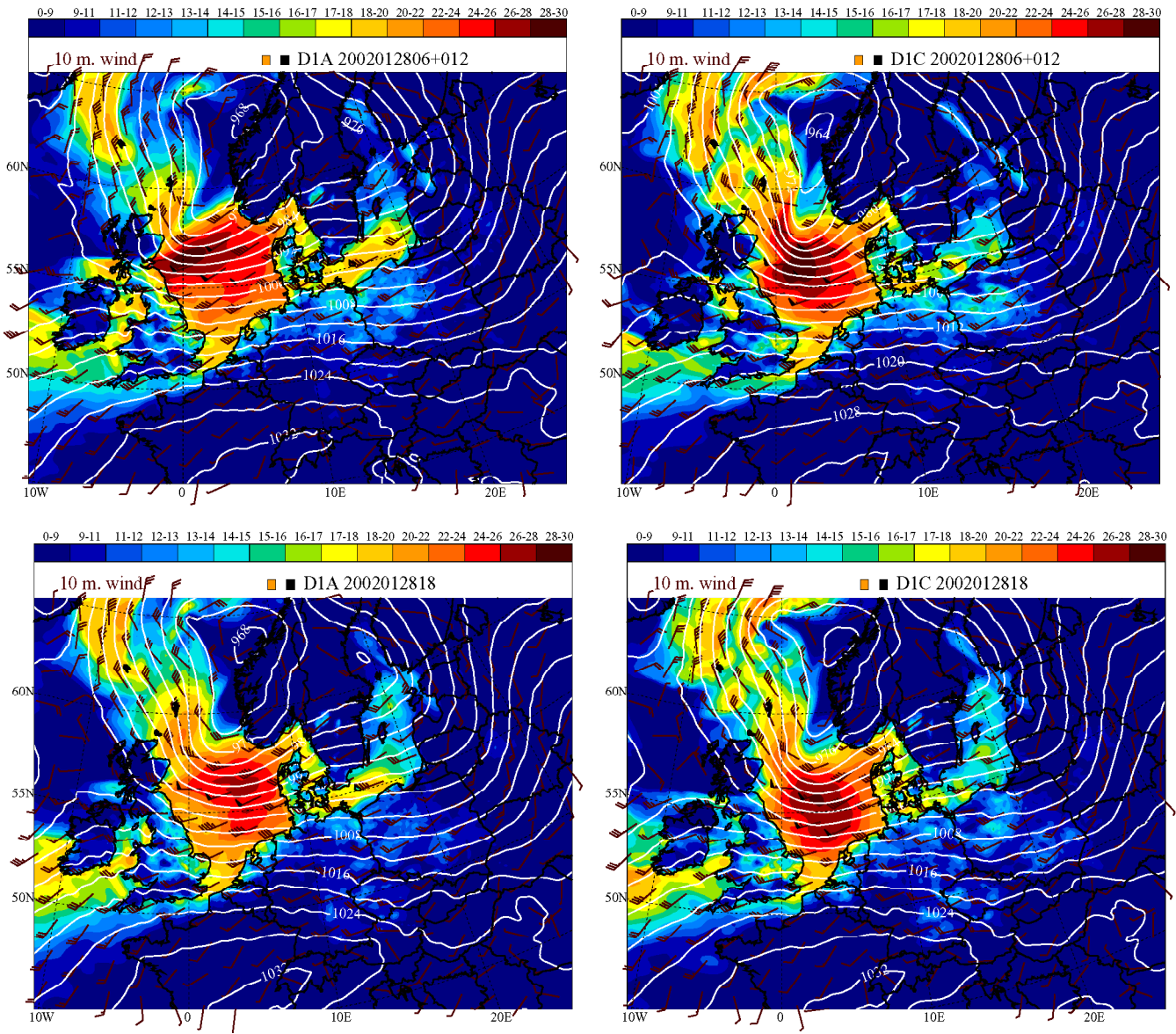


**Figure 17:** Operational DMI-HIRLAM-E (left) and new DMI-HIRLAM-E (right) mslp and 10 m wind speed valid on 18 UTC January 28, 2002. Upper row is 12 hour forecasts and lower row the verifying analyses.

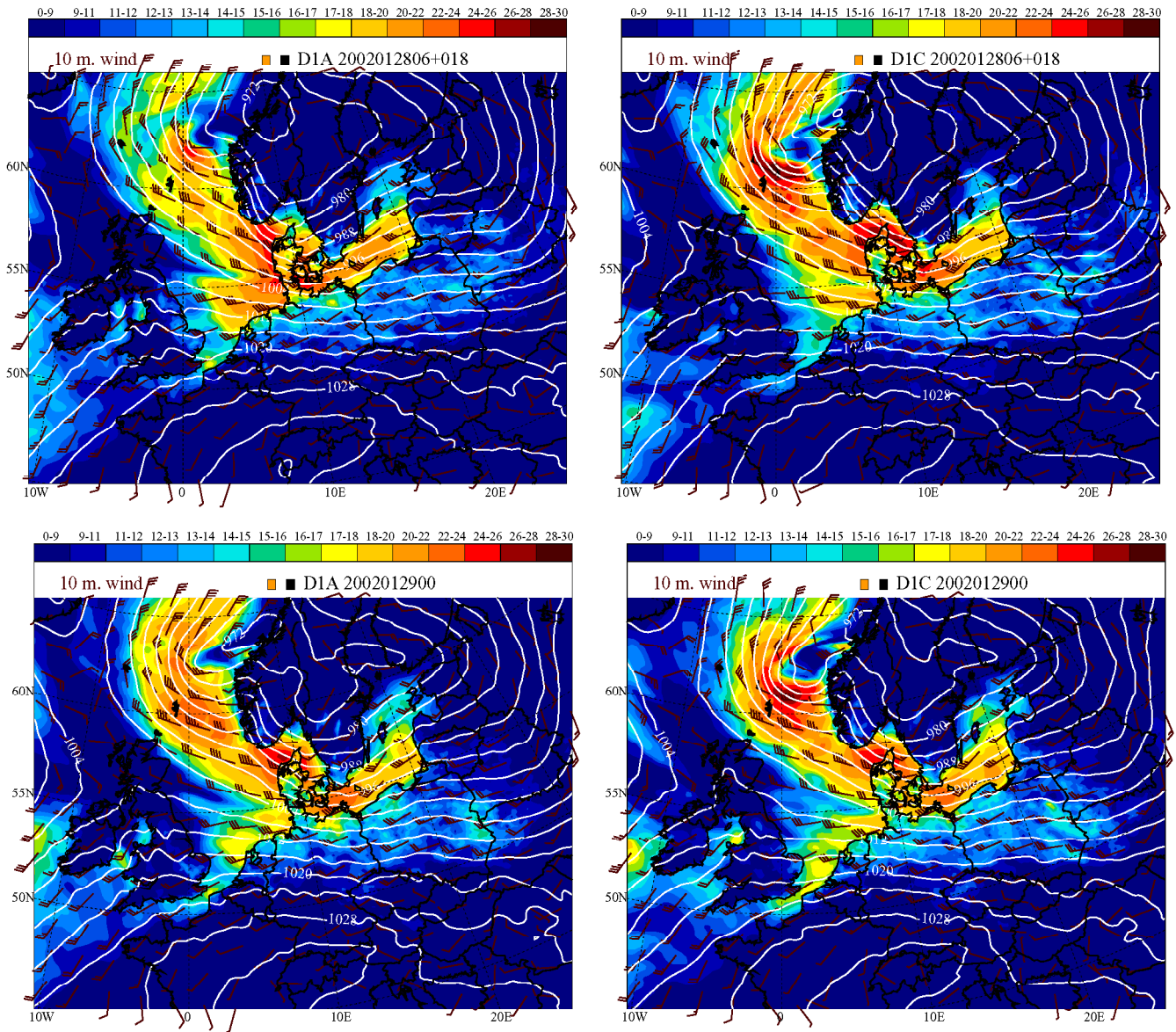


**Figure 18:** Operational DMI-HIRLAM-E (left) and new DMI-HIRLAM-E (right) mslp and 10 m wind speed valid on 00 UTC January 29, 2002. Upper row is 18 hour forecasts and lower row the verifying analyses.

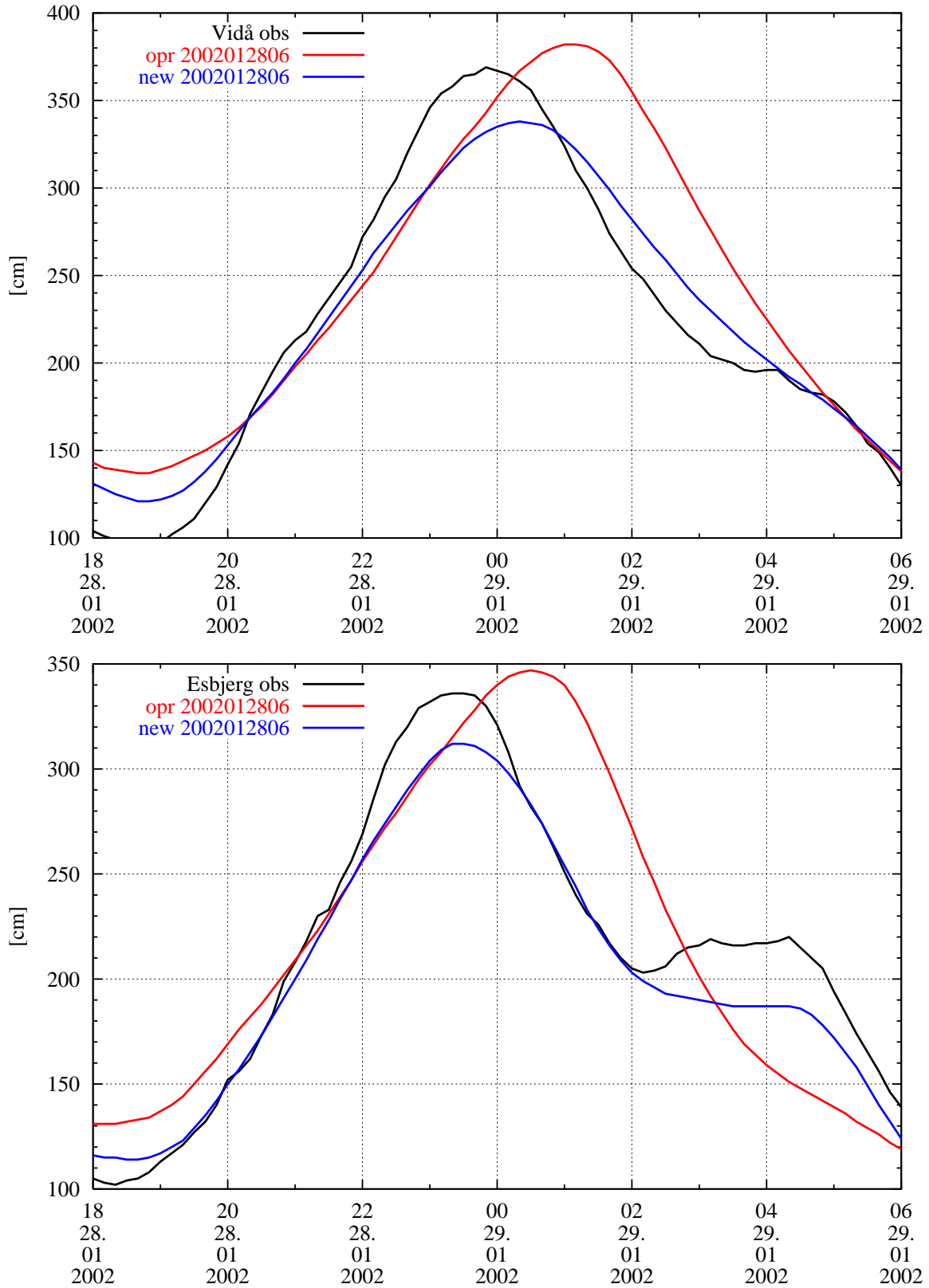


**Figure 19:** Mike21 runs starting from 06 UTC January 28 for Vidå (upper) and Esbjerg (lower) stations.

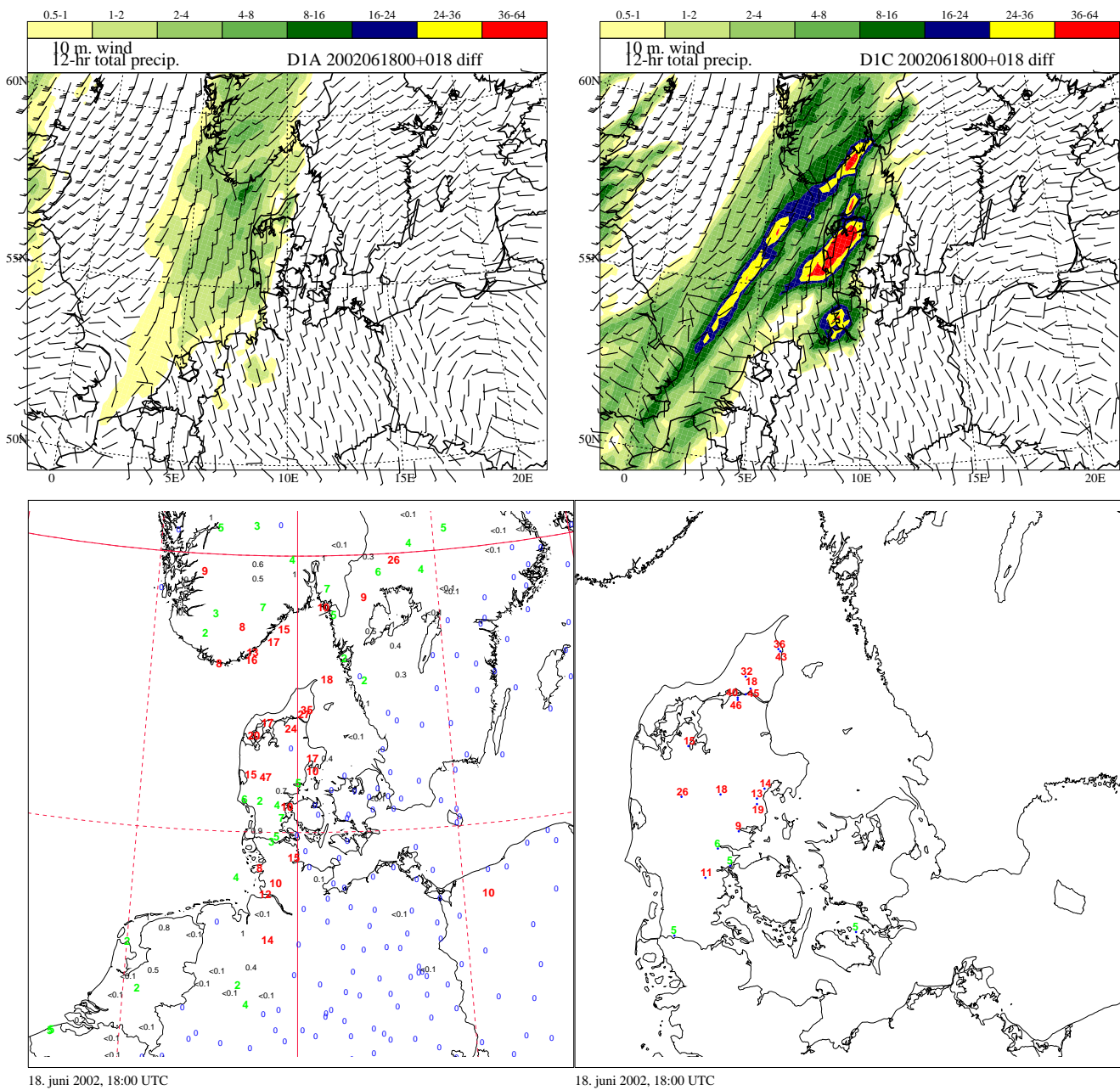


**Figure 20:** DMI-HIRLAM-E (D1A, upper left) and DMI-HIRLAM-E-new (D1C, upper right) forecasted (6 h-18 h forecasts) 12h accumulated precipitation valid on 18 UTC June 18. At the bottom observed 12 h accumulated precipitation up to 18 UTC June 18 (SYNOPSIS stations to the left and values from SVK stations to the right). Only values greater than or equal 2 mm are shown for SVK stations.

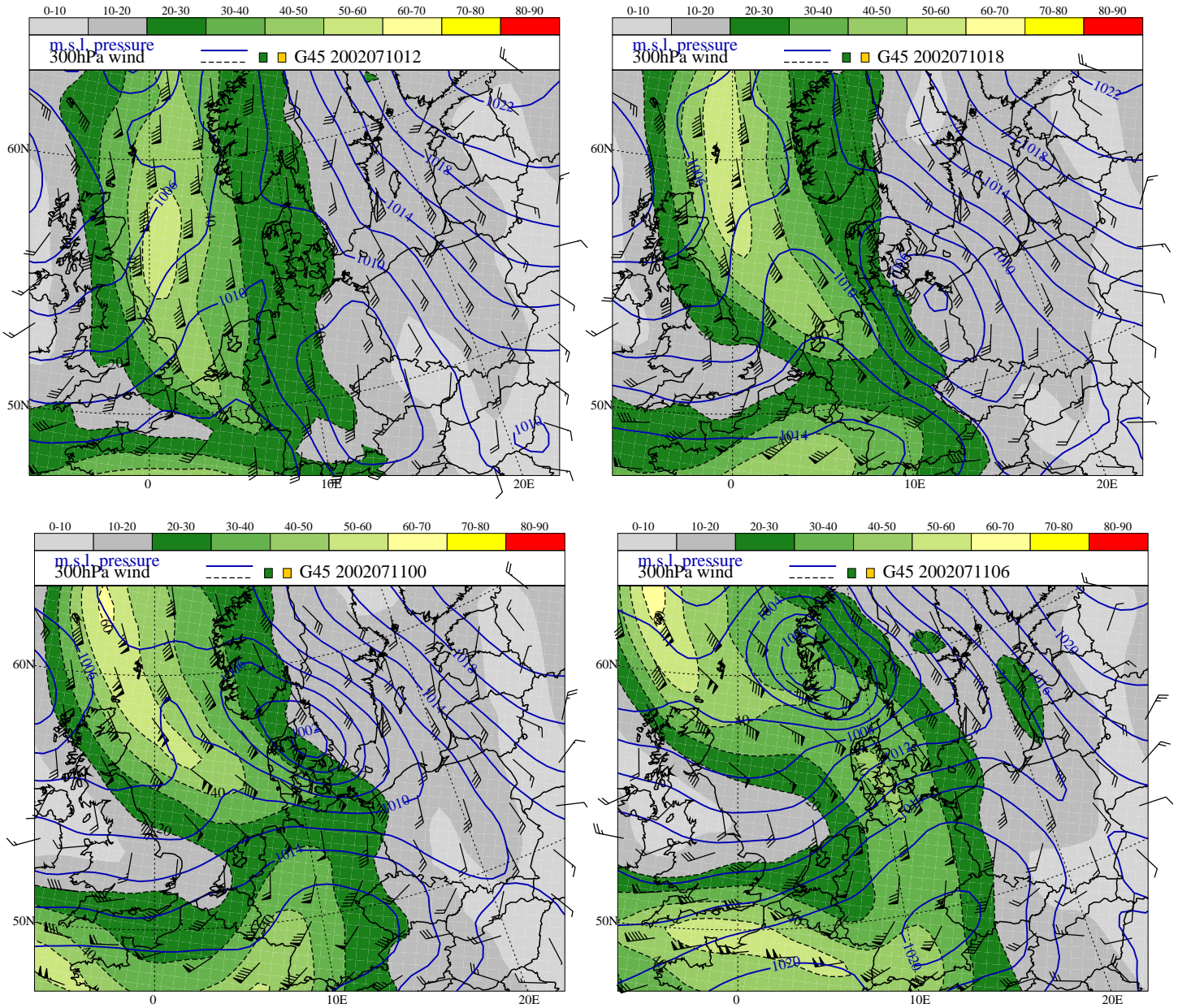


**Figure 21:** Operational DMI-HIRLAM-G ‘analyses’ of mslp and wind at 300 hPa valid at a) 12 UTC (upper left), b) 18 UTC (upper right), c) 00 UTC (lower left), and d) 06 UTC (lower right) 10-11 July 2002. Contour interval for mslp is 2 hPa. Contour interval for wind speed is  $10 \text{ m s}^{-1}$ , minimum contour is  $20 \text{ m s}^{-1}$ . Wind arrows are WMO standard.



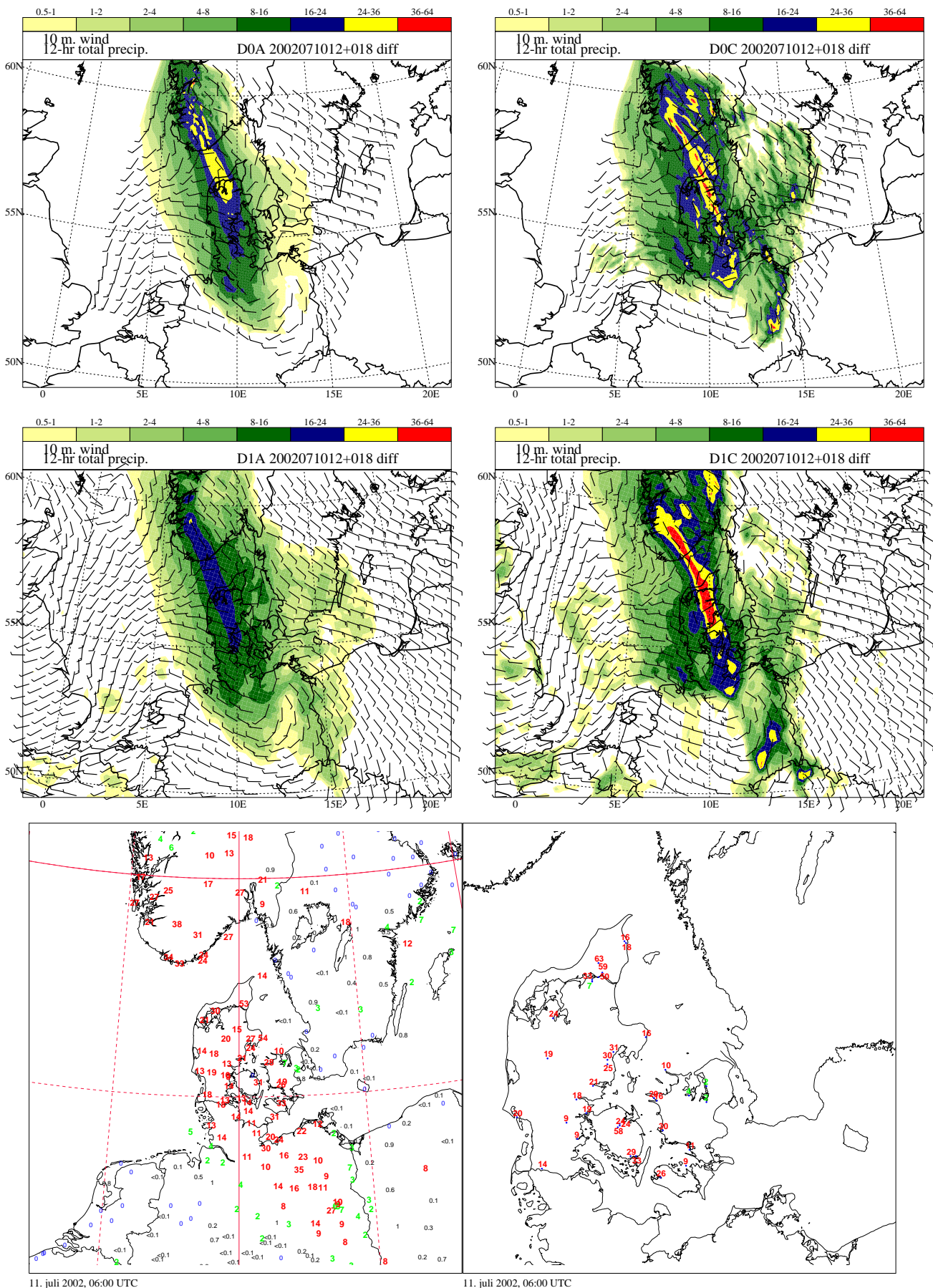


**Figure 22:** DMI-HIRLAM-D (D0A, upper left), DMI-HIRLAM-D-new (D0C, upper right), DMI-HIRLAM-E (D1A, middle left) and DMI-HIRLAM-E-new (D1C, middle right) forecasted (6 h-18 h forecasts) 12 h accumulated precipitation valid on 06 UTC July 11. At the bottom observed 12 h accumulated precipitation up to 06 UTC July 11 (SYNOP stations to the left and values from SVK stations to the right). Only values greater than or equal 2 mm are shown for SVK stations.

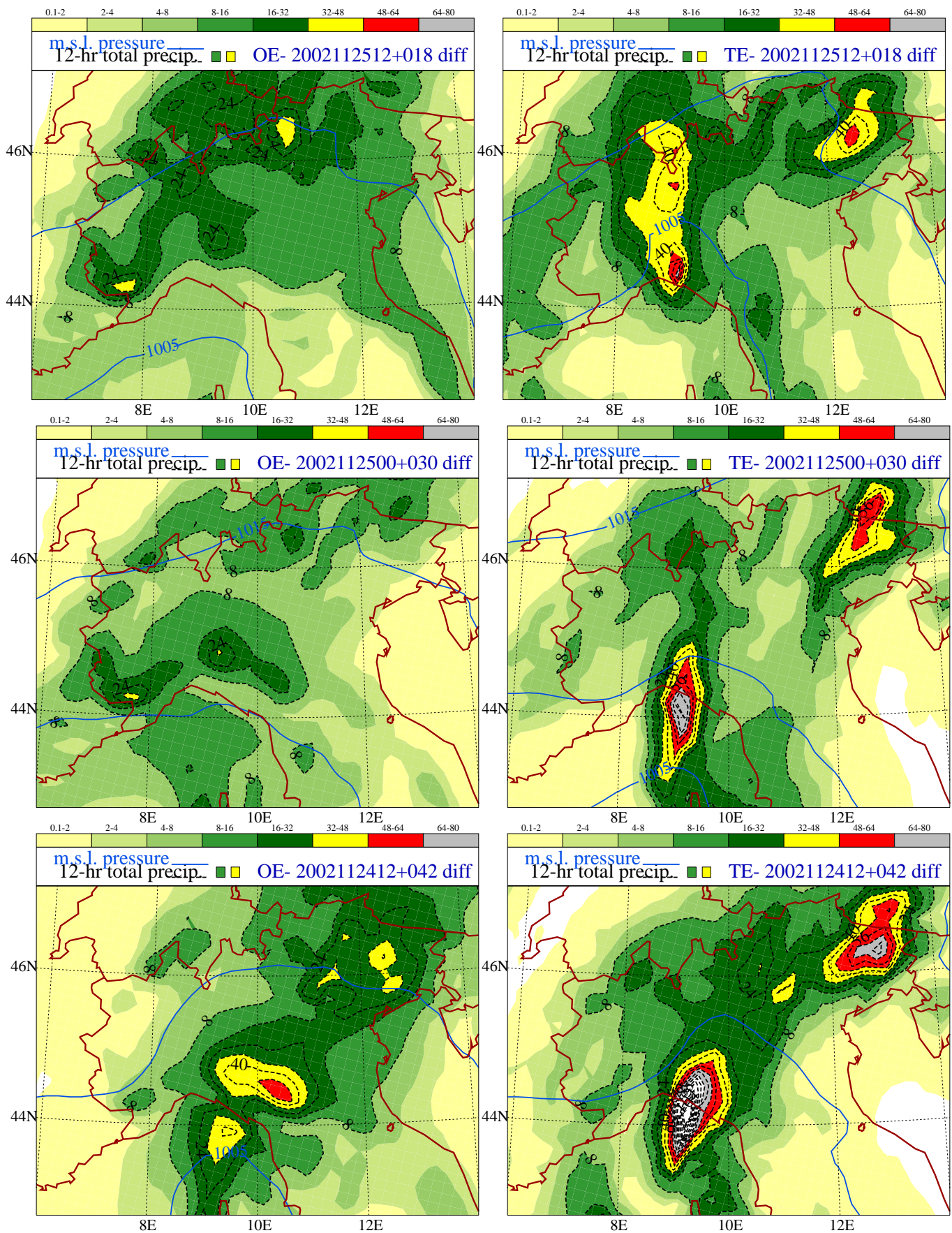
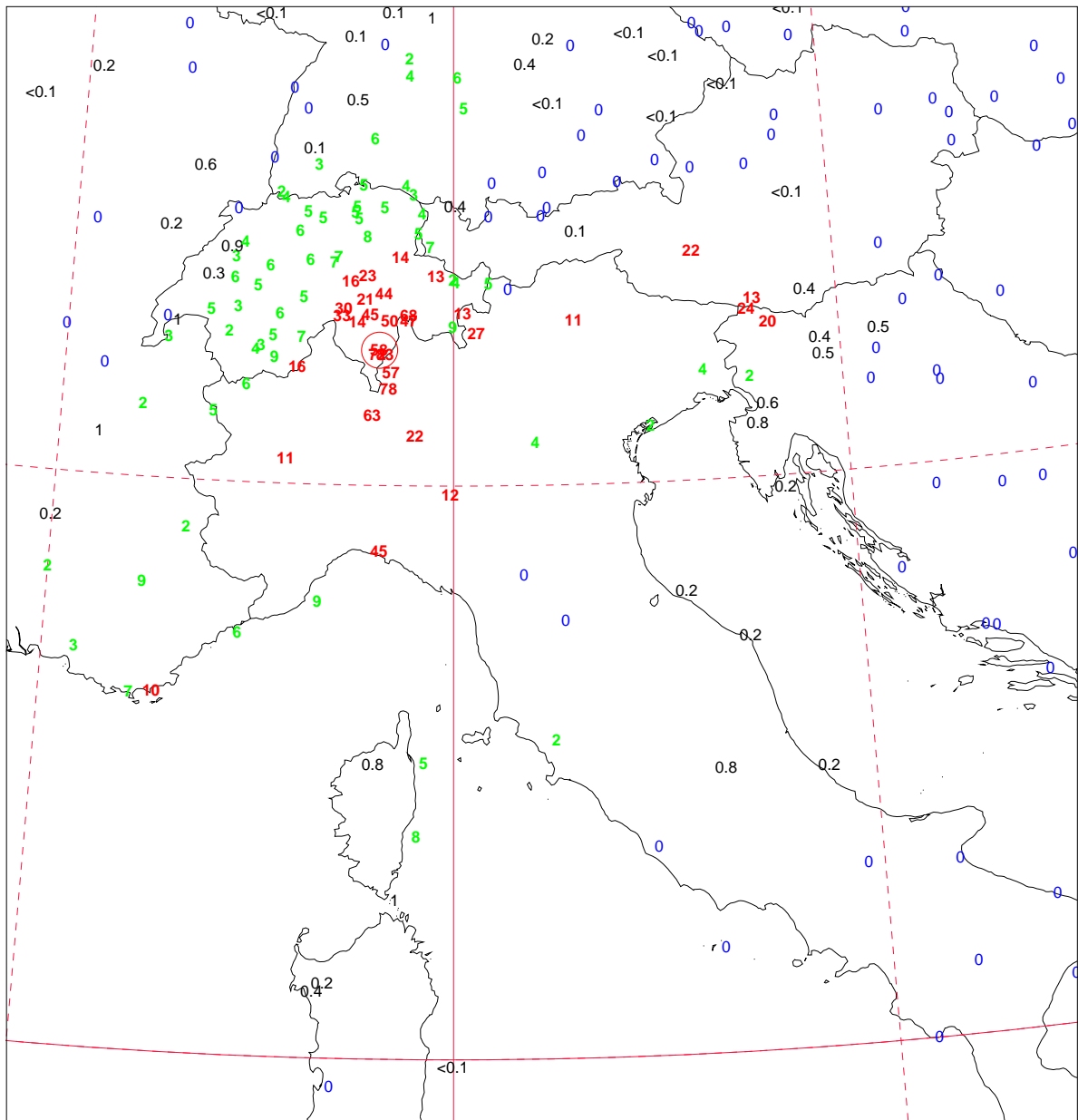


**Figure 23:** The operational DMI-HIRLAM-E (OE, left) and DMI-HIRLAM-E-new (TE, right) forecasted (6 h-18 h forecasts upper, 18 h-30 h middle and 30 h-42 h bottom) 12 h accumulated precipitation valid on 06 UTC November 26 2002.



26. november 2002, 06:00 UTC

**Figure 24:** Observed 12 h accumulated precipitation up to 06 UTC November 26 2002 from SYNOP stations. Values greater than or equal 10 mm are shown with red color, values greater than or equal 2 mm and less than 10 mm are green and values of 0 mm is blue. The 3 values inside the red circle are 53 mm (CIMETTA), 72 mm (LOCARNO-MONTI) and 83 mm (LOCARNO-MAGADINO).